TOPICAL REVIEW — ZnO-related materials and devices

Review of flexible and transparent thin-film transistors based on zinc oxide and related materials[*]

Yong-Hui Zhang(张永晖)[1],   Zeng-Xia Mei(梅增霞)[1,†],   Hui-Li Liang(梁会力)[1],   and   Xiao-Long Du(杜小龙)[1,2,‡]

[1]Key Laboratory for Renewable Energy, Beijing National Laboratory for Condensed Matter Physics, Institute of Physics,
Chinese Academy of Sciences, Beijing 100190, China
[2]School of Physical Sciences, University of Chinese Academy of Sciences, Beijing 100190, China

Flexible and transparent electronics enters into a new era of electronic technologies. Ubiquitous applications involve wearable electronics, biosensors, flexible transparent displays, radio-frequency identifications (RFIDs), etc. Zinc oxide (ZnO) and relevant materials are the most commonly used inorganic semiconductors in flexible and transparent devices, owing to their high electrical performances, together with low processing temperatures and good optical transparencies. In this paper, we review recent advances in flexible and transparent thin-film transistors (TFTs) based on ZnO and relevant materials. After a brief introduction, the main progress of the preparation of each component (substrate, electrodes, channel and dielectrics) is summarized and discussed. Then, the effect of mechanical bending on electrical performance is highlighted. Finally, we suggest the challenges and opportunities in future investigations.

Keywords: zinc oxide, flexible electronics, transparent electronics, thin-film transistors

PACS: 73.61.Ga, 85.30.Tv

DOI: 10.1088/1674-1056/26/4/047307

1. Introduction

The last thirteen years have witnessed the rise of flexible and transparent electronics. Since Hoffman *et al*. demonstrated the first fully transparent zinc oxide thin-film transistor (ZnO TFT) in 2003,[1] numerous important researches have been reported.[2–21] The typical applications involve active-matrix flexible or transparent displays, logic circuits, electronic skins, bio-sensors, and wearable devices. Owing to their mechanical flexibilities, optical transparencies, light weights, low production costs, low power consumptions and, above all, high electrical performances, these devices have drawn broad interest in both academy and industrial circles. A wide range of diverse applications of flexible and transparent TFTs based on ZnO related materials are illustrated in Fig. 1.
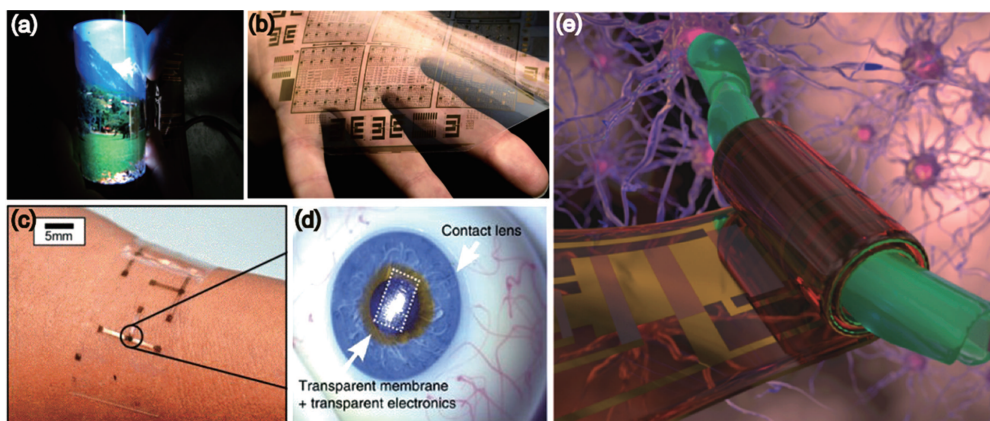

Fig. 1. (color online) Versatile applications of ZnO related TFTs: (a) 6.5-in (1 in = 2.54 cm) flexible full-color display driven by indium gallium zinc oxide (IGZO) TFTs.[6] (b) Flexible transparent IGZO circuits.[7] (c) Electronic skin based on IGZO TFT.[22] (d) Smart contact lens based on IGZO TFTs.[23] (e) Biomimetic neuronal microelectronics based on IGZO TFT.[16]

Organic and hydrogenated amorphous silicon (a-Si:H) TFTs have also been demonstrated but their applications are limited by the low mobility of the conductive channel. ZnO and relevant materials have thus emerged as promising candidates for channel materials in flexible and transparent TFTs since the advent of this subject field in 2003–2004.[1,4] Compared with other inorganic wide bandgap semiconductors, such as gallium nitride (GaN) and silicon carbide (SiC), the

http://iopscience.iop.org/cpb   http://cpb.iphy.ac.cn

ZnO materials for flexible devices have a great advantage, i.e., their low synthesis temperatures, which is exactly the most important requirement in flexible device fabrication process.[24] (For details, see Section 2.) The biocompatibilities of ZnO materials also make them perfectly desirable for medical and health-care applications as shown in Figs. 1(c)–1(e).

In addition, the feasibility of modulating the electrical properties via doping or alloying with other elements offers the opportunities to adjust device performances and thus their own diverse functionalities. The most commonly used alloys are indium zinc oxide (IZO), IGZO, zinc tin oxide (ZTO), zinc indium tin oxide (ZITO), and magnesium zinc oxide (MZO). Listed in Table 1 are some of the state-of-the-art flexible transparent TFTs based on versatile ZnO and relevant materials in the past 6 years.

Table 1. Some of the state-of-the-art flexible transparent TFTs based on ZnO and relevant materials in the period of 2010–2016. ("–" means not mentioned or not clear in the literature).

Material	Technique	$(T_{dep.}/T_{post.})/(°C)$	Substrate	Dielectric	$\mu/(cm^2 \cdot V^{-1} \cdot s^{-1})$	On/off	Reference	Year
ZnO	spin-coating	–/135	PEN	$RSiO_{1.5}$	0.07	10^4	Fleischhaker et al.[25]	2010
ZnO	ALD	150/–	PI	Al_2O_3	3.07	10^2	Cherenack et al.[26]	2010
ZnO	sputtering	RT/350	PDMS	SiO_2	1.3	10^6	Park et al.[27]	2010
ZnO	hydrothermal	90/100	PET	PMMA	7.53	10^4	Lee et al.[28]	2010
ZnO	spin-coating	RT/200	PI	SiO_2	0.35	10^6	Song et al.[29]	2010
ZnO	PEALD	200/–	PI	Al_2O_3	20	10^7	Zhao et al.[30]	2010
IGZO	sputtering	RT/–	PI	Al_2O_3	12.85	10^6	Cherenack et al.[26]	2010
IGZO	sputtering	–/–	PET	BST/PMMA	10.2	10^6	Kim et al.[31]	2010
IGZO	PLD	RT/–	PET	parylene	3.2	10^7	Nomura et al.[32]	2010
IGZO	sputtering	RT/200	PI	HfLaO	22.1	10^5	Su et al.[33]	2010
ZITO	PLD	–/–	PET	Ta_2O_5/SiO_x	20	10^5	Liu et al.[34]	2010
ZITO	PLD	RT/–	PET	v-SAND	110	10^4	Liu et al.[35]	2010
ZITO	sputtering	RT/–	polyarylate	Al_2O_3	16.93	10^9	Cheong et al.[36]	2010
ZnO	spin-coating	RT/MW140	PES	SiO_2	0.57	10^3	Jun et al.[37]	2011
ZnO	spin-coating	–/150	PES	hybrid	0.142	10^4	Jung et al.[38]	2011
IGZO	sputtering	200/220	PI	SiO_2	19.6	10^9	Mativenga et al.[39]	2011
IGZO	sputtering	–/150	PEN	Al_2O_3	17	10^8	Tripathi et al.[7]	2011
IGZO	sputtering	200/220	PI	SiO_2	19	10^9	Mativenga et al.[39]	2011
IGZO	–	–/–	PI	Al_2O_3	13.7	10^7	Kinkeldei et al.[40]	2011
IGZO/IZO	sputtering	40/200	PEN	SiO_2	18	10^9	Mars et al.[41]	2011
IGZO	sputtering	RT/–	PI	Al_2O_3	14.5	10^7	Münzenrieder et al.[42]	2012
IGZO	sputtering	RT/–	PEN	PVP	0.43	10^5	Lai et al.[43]	2012
IGZO	sputtering	RT/–	PU	Al_2O_3	9.36	10^5	Erb et al.[44]	2012
IGZO	sputtering	RT/–	PI	PVP	3.6	10^4	Kim et al.[45]	2012
IGZO	sputtering	–/PN254 nm	PAR	Al_2O_3	7	10^8	Kim et al.[46]	2012
ZnO	sputtering	100/–	PET	HfO_2	7.95	10^8	Ji et al.[47]	2013
ZnO	spin-coating	–/200	PET	c-PVP	0.09	10^5	Kim et al.[48]	2013
ZnO	printing	–/250	PI	ion-gel	1.67	10^5	Hong et al.[49]	2013
ZnO	spin-coating	–/160	PEN	Al_2O_3-ZrO_2	5	10^4	Lin et al.[50]	2013
IZO	spin-coating	RT/280	PI	Zr-Al_2O_3	51	10^4	Yang et al.[51]	2013
IZO	sputtering	RT/RT	PET	SiO_2	65.8	10^6	Zhou et al.[52]	2013
IZO:F	spin-coating	RT/200	PEN	Al_2O_3	4.1	10^8	Seo et al.[53]	2013
IGZO	sputtering	RT/110	PET	c-PVP	10.2	10^6	Hyung et al.[54]	2013
IGZO	sputtering	–/–	PC	$Y_2O_3/TiO_2/Y_2O_3$	32.7	10^6	Hsu et al.[55]	2013
IGZO	sputtering	–/–	PC	$GeO_2/TiO_2/GeO_2$	8	10^7	Hsu et al.[56]	2013
IGZO	sputtering	RT/RT	PC	$SiO_2/TiO_2/SiO_2$	76	10^5	Hsu et al.[57]	2013
IGZO	sputtering	RT/–	PI	Al_2O_3	7.3	10^9	Münzenrieder et al.[58]	2013
IGZO	sputtering	RT/–	PI	Al_2O_3	8.3	10^8	Münzenrieder et al.[59]	2013
IGZO	sputtering	RT/–	PI	Al_2O_3	18.3	10^8	Zysset et al.[60]	2013
IGZO	printing	–/–	PDMS	SiO_2	15	10^6	Sharma et al.[61]	2013
GNS/IGZO	spin-coating	–/500	thin glass	Ta_2O_5	23.8	10^6	Dai et al.[62]	2013
ZnO	sputtering	–/MW	PES	Al_2O_3	1.5	10^6	Park et al.[63]	2014
IZO	spin-coating	RT/350	PI	K-PIB	4.1	10^5	Wee et al.[64]	2014
IGZO	sputtering	–/–	PI	Al_2O_3/SiO_2	9	10^7	Chen et al.[65]	2014
IGZO	sputtering	–/160	PEN	Al_2O_3	11.2	10^9	Xu et al.[66]	2014
IGZO	sputtering	150/150	PEN	Al_2O_3	12.87	10^9	Xu et al.[67]	2014
IGZO	sputtering	RT/–	PEN	nanocomposite	5.13	10^5	Lai et al.[68]	2014
IGZO	sputtering	RT/250	PI	Al_2O_3	14.88	10^8	OK et al.[69]	2014

Table 1. (*Continued*).

Material	Technique	$(T_\text{dep.}/T_\text{post.})/(^\circ\text{C})$	Substrate	Dielectric	$\mu/(\text{cm}^2\cdot\text{V}^{-1}\cdot\text{s}^{-1})$	On/off	Reference	Year
IGZO	sputtering	RT/190	PEN	SiO_2	8	10^7	Nakajima *et al.*[70]	2014
IGZO	spin-coating	RT/350	PI	Al_2O_3	84.4	10^5	Rim *et al.*[71]	2014
IGZO	sputtering	–/–	parylene	Al_2O_3	11	10^4	Salvatore *et al.*[23]	2014
IGZO	sputtering	RT/–	PI	Al_2O_3	7.5	10^7	Petti *et al.*[72]	2014
IGZO	sputtering	RT/–	PI	Al_2O_3	10.5	10^8	Münzenrieder *et al.*[73]	2014
IGZO	sputtering	–/300	thin glass	Si_3N_4	9.1	10^8	Lee *et al.*[74]	2014
ZnO	PEALD	200/–	PI	Al_2O_3	12	10^8	Li *et al.*[75]	2015
IZO	sputtering	–/–	PET	SiO_2	12	10^5	Liu *et al.*[76]	2015
IGZO	sputtering	–/–	–	Si_3N_4	6.5	10^6	Kim *et al.*[77]	2015
IGZO	sputtering	RT/–	PI	Al_2O_3/ SiO_2	4.93	5	Honda *et al.*[78]	2015
IGZO	spin-coating	–/PN254 nm	PI	ZAO	11	10^9	Jo *et al.*[79]	2015
IGZO	sputtering	–/160	PEN	SiO_2	7	10^7	Motomura *et al.*[80]	2015
IGZO	sputtering	RT/200	PDMS	P(VDF-TrFE)	21	10^7	Jung *et al.*[81]	2015
IGZO	sputtering	RT/–	PI	Al_2O_3	17	10^5	Karnaushenko *et al.*[16]	2015
IGZO	sputtering	RT/150	PVA	SiO_2/Si_3N_4	10	10^6	Jin *et al.*[82]	2015
IGZO	sputtering	RT/180	PEN	Al_2O_3	15.5	10^9	Park *et al.*[83]	2015
IGZO	sputtering	–/–	PI	Al_2O_3	0.2	10^4	Petti *et al.*[84]	2015
IGZO	sputtering	–/180	PEN	Si_3N_4	13	10^8	Tripathi *et al.*[85]	2015
IGZO/TO	sputtering	–/–	PC	TiO_2/HfO_2	61	10^5	Hsu *et al.*[86]	2015
ZnO	sputtering	–/225	PI	HfO_2	1.6	10^6	Li *et al.*[87]	2016
ZnO	sputtering	RT/RT	PEN	Al_2O_3	11.56	10^8	Zhang *et al.*[88]	2016
IZO	sputtering	–/300	PI	Al_2O_3	6.64	10^7	Zhang *et al.*[89]	2016
IZO	SCS	275/–	polyester	Al_2O_3/ ZrO_2	3.9/6.2	10^4	Wang *et al.*[90]	2016
IGZO	sputtering	RT/–	PI	SiO_2	12	10^7	Park *et al.*[91]	2016
IGZO	sputtering	RT/200	PDMS	P(VDF-TrFE):PMMA	0.35	10^4	Jung *et al.*[92]	2016
IGZO	spin-coating	–/ PN254 nm	PI	Al_2O_3	5.41	10^8	Kim *et al.*[93]	2016
IGZO	sputtering	–/–	PES	Al_2O_3	71.8	10^8	Oh *et al.*[94]	2016
ZTO	Inkjet printing	30/300	PI	ZrO_2	0.04	10^3	Zeumault *et al.*[95]	2016
ZITO	sputtering	300/200	PI	SiO_2	32.9	10^9	Nakata *et al.*[96]	2016

Besides TFTs, the operation of a flexible transparent circuit also needs high-performance thin film diodes. However, research on flexible transparent diodes is quite limited despite the great progress made in TFTs as shown in Table 1. The limited reports can be categorized into 5 types as follows. (i) The pn heterojunction diode.[97–102] As most of the wide-bandgap semiconductors are n-type conductive, a proper p-type wide-bandgap material must be chosen wisely to form a large built-in potential barrier. (ii) Schottky junction diode.[103–106] The values of electron affinity (χ) of most wide-bandgap materials are all more than 4 eV, thus only a small Schottky barrier height (SBH) could be formed with non-noble metals. (iii) Metal-insulator-semiconductor (MIS) diode.[107] As in Schottky diode, a large difference between metal work function (Φ_M) and semiconductor affinity (χ) is necessary to achieve a large rectification ratio. (iv) Metal–insulator–metal (MIM) diode.[108,109] Actually, it is not easy for MIM diodes to be applied to transparent circuits because of the difficulties in finding two kinds of transparent electrodes with large work function difference. (v) Self-switching diode (SSD).[110] Besides small rectification ratio, this kind of device involves nanofabrication process, which may bring high costs and challenges in technological compatibility. Zhang *et al.* recently demonstrated high-performance flexible fully transparent ZnO diodes with a high rectification ratio of 10^8 by using a diode-connected TFT architecture as shown in Fig. 2(a).[88] The device fabrication procedure is the same as that for standard TFTs (Fig. 2(b)). Both of the devices on polyethylene naphthalate (PEN) and quartz substrates are optically transparent (see the inset in Fig. 2(c)), with the whole devices (including the substrates) exhibiting a transmittance over 80% in full visible spectral range (Fig. 2(c)). Most importantly, the devices exhibit a high rectification ratio of 5×10^8 (Fig. 2(d)) under flat and bent states (see the inset in Fig. 2(d)), which is 3–4 orders larger than those of conventional junction diodes. This work has broadened the application scope of flexible transparent TFTs and provided a solution to flexible fully transparent diodes which may be used for reference to flexible transparent TFTs based on other materials.

Owing to the rapid developments of science and technology in flexible transparent electronics, many wonderful products are very close to achieving commercial-productions.[111,112] In fact, IGZO panels have already been used in iPad Air and iPad Pro products, and Apple is considering IGZO panel for its new iPhone in late 2017. As for flexible transparent display and other more applications, there are still difficulties before desirable products come into use. In this regard, the present review aims at summarizing recent advances in flexible and transparent TFTs based on ZnO and relevant materials, and discussing the major challenges in

device fabrication and mechanical strain effects. Finally, we propose several issues to be considered for further investigations. Since there are plenty of reviews on oxide semiconductor TFTs,[11,12,17–21,113,114] to avoid repetition, this review will specifically focus on ZnO and relevant materials and emphasize the novel device physics and technical problems which are only present in flexible and transparent ZnO field-effect transistors.
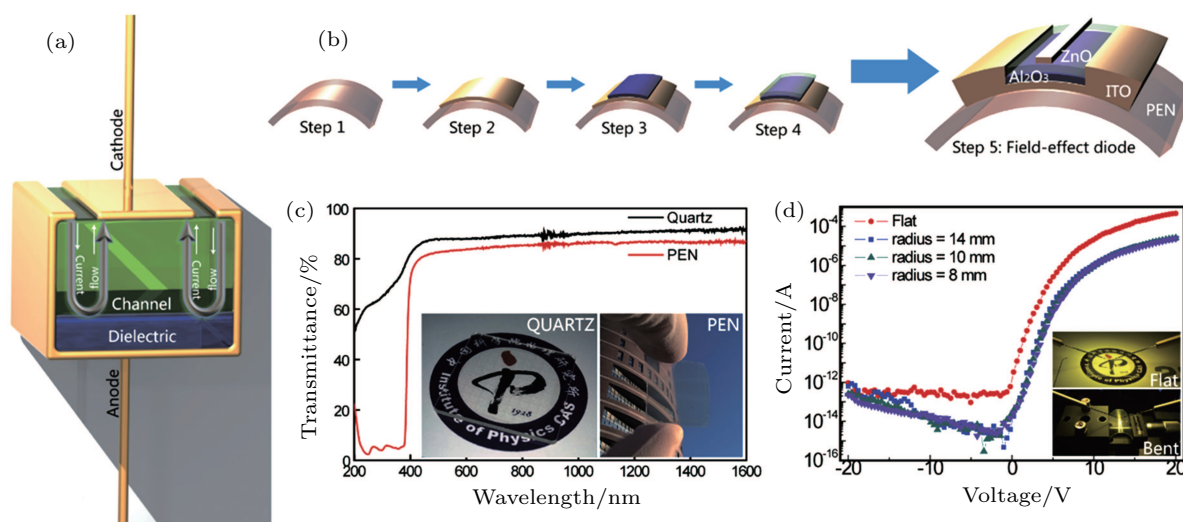

Fig. 2. (color online) Device structure and performance of flexible transparent ZnO diode. (a) Conceptualized structure diagram, which features two-terminal configuration. (b) Fabrication procedure of field-effect diode. (c) Optical transmittance spectra of devices on glass and PEN substrates with transmittance over 80% in a visible spectral range. The insets show the photographs of these two devices. (d) Current–voltage (I–V) characteristics of field-effect diode with a high rectification ratio of 5×10^8 while flat and bent. Insets show the photographs of device under test.[88]

2. Device fabrication

TFTs fabricated on flexible substrates are lightweight, low costed, rugged, flexible, foldable, twistable or even stretchable. However, they are also vulnerable to ambient environment. Therefore, device fabrication and characterization processes may be quite different compared with conventional case on rigid substrates, such as glass and silicon.[115,116] The most serious problem associated with flexible and transparent (polymer) substrates is the changes of their dimensions, which would bring difficulties to sequential alignment. Besides, the mismatch between substrates and films during dimension change would cause strain in the film and thus degrade the material quality, or even cracks and delamination which would cause permanent failure. This undesirable dimension change comes from the large differences in coefficient of thermal expansion (CTE), elastic modulus and toughness between the polymer substrates and functional films on them. Other issues with polymer substrates are surface roughness, chemical stability and gas permeability, which will be discussed in Subsection 2.1. Afterwards, the device physics and technical process in preparing channel, dielectric and electrodes layers will be discussed in Subsections 2.2, 2.3, and 2.4, respectively.

2.1. Flexible substrates

The properties of polymer substrates will affect material quality and carrier transportation behavior and limit maximum fabrication temperature, and thus are of great impor-

tance for the flexible transparent devices. As shown in Fig. 3, according to the servicing temperature or glass transition temperature (T_g), the polymer substrates can be categorized into three types: conventional polymers ($T_g < 100$ °C), common high-temperature polymers ($100 \leq T_g < 200$ °C) and high-temperature polymers ($T_g \geq 200$ °C).[117] The most commonly used polymer substrates in the literature include polyimide (PI), polyarylate (PAR), polyethylene terephthalate (PET), PEN, polyethersulfone (PES), polycarbonate (PC), polyetheretherketone (PEEK), polydimethylsiloxane (PDMS), etc.
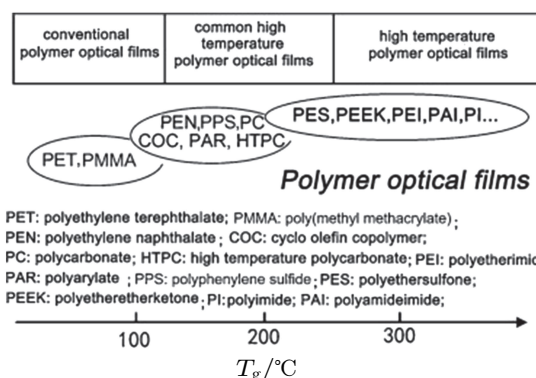

Fig. 3. Classification of polymer optical films. According to the servicing temperature, polymer films can be categorized into 3 types: conventional polymers ($T_g < 100$ °C), common high-temperature polymers ($100 \leq T_g < 200$ °C) and high-temperature polymers ($T_g \geq 200$ °C).[117]

In Table 2 listed are the basic properties of PI, PEN, and PET for each of the three kinds of polymer substrates which are currently widely used.

Table 2. Basic properties of four commonly used flexible transparent substrates.

Material	T_g/°C	CTE/(ppm·°C^{-1})	λ_c/nm	Chemical resistance	Surface roughness
PI	300	12	500	Good	Good
PEN	120	20	380	Good	Moderate
PET	80	33	300	Good	Moderate
PDMS	−120	301	200	Good	Poor

The PI substrate has the highest T_g, smallest CTE and surface roughness among all of the flexible substrates. In addition, it also shows good chemical stability in acid, alkali and organic solvents. Although the cut-off wavelength (λ_c) is in the visible range, which means that the PI substrates have deep color and poor optical transmittance as can be seen in Fig. 4, the colorless and optically transparent polyimide (CPI) films have been developed recently[117] and used in IGZO TFT fabrication.[118] In the case that the cost is not a problem, the CPI substrates will be the best choice for flexible transparent electronics. The PET substrate has excellent optical transparency and short λ_c (Fig. 4), and is currently widely used as the protection layers in various liquid crystal displayers (LCDs), such as televisions, computers and cellphones. The major disadvantage of PET for its use in flexible transparent TFTs is its relatively low servicing temperature ($T_g \approx 80$ °C), which may bring challenges to device fabrication, integration and operation. The PEN substrate has higher servicing temperature ($T_g \approx 120$ °C) than PET, but, as a compromise, it appears slightly white color as can be seen in Fig. 4. The PDMS substrate was recently used in flexible TFTs.[27,61,81,92,119] Besides the high optical transmittance and short λ_c, PMDS also features small elastic modulus ($E \approx 5$ MPa), which makes PDMS the perfect substrate for the emerging stretchable electronics.[17,27,61,92,120–122] It is worth noting that ultra-thin (25 μm–100 μm) flexible glass, such as Willow by Corning company,[123] is also regarded as a promising flexible substrate for flexible transparent electronics with considering its higher servicing temperature (∼ 500 °C), good resistance to scratch and higher optical transmittance. However, up to now, few researches on flexible glass have been reported in the literature.[62,74]
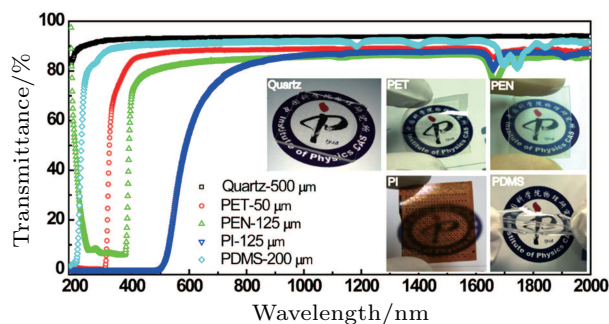

Fig. 4. (color online) Optical transmittance spectra of four commonly used flexible transparent substrates (PI, PET, PEN & PDMS) in comparison with rigid quartz. Insets shows the actual photographs of the substrates

To reduce the surface roughness and gas permeability, and to increase the chemical resistance and adhesion to the film, a barrier layer or encapsulation is often involved onto the substrate.[69,83,124] The commonly used encapsulation materials are Al_2O_3,[125,126] Si_3N_4,[58,127] and SiO_2,[27,82] which are electrical insulating and easy to grow by chemical vapor deposition with perfect coverage ratio. Encapsulations of stacked layer have also been reported.[67,69,91]

2.2. Channel layers

Whatever the substrate is, the device performance usually depends on channel layer, especially within 1 nm–2 nm from the interfacial layer. The electron mobility, electron concentration, density of state and interfacial charge would directly influence the field-effect mobility, on/off ratio, sub-threshold swing and turn-on voltage. In this part, we summarize the properties of ZnO channel layer that only appears in flexible transparent device.

As described in Subsection 2.1, limited by the utilized flexible substrate, the processing temperature cannot exceed T_g, which could be as low as 80 °C. At such a low synthesis temperature, the materials usually appear to be polycrystalline or amorphous. In conventional semiconductors, such as silicon whose conduction band minimum (CBM) and valence band maximum (VBM) are composed of anti-bonding ($sp^3\sigma^*$) and bonding ($sp^3\sigma$) states of Si sp^3 orbitals and whose band gap is formed by splitting the σ^*–σ energy levels (Fig. 5(a)), the carrier transport properties depend critically on the chemical bonding direction (Fig. 5(b)). This is the reason for the degradation of electron mobility in amorphous silicon ($\mu < 2$ cm^2·V^{-1}·s^{-1}) compared with crystalline silicon ($\mu \approx 1500$ cm^2·V^{-1}·s^{-1}). In contrast to silicon, ZnO has very strong ionicity and electrons transfer from zinc to oxygen atoms. The electronic structure is formed by rasing the electronic level in zinc and lowering the electronic level in oxygen through the Madelung potential as shown in Fig. 5(c). As a result, the CBM in ZnO is primarily contributed to by the unoccupied spherically symmetric Zn 4s orbitals and the VBM is primarily determioned by the fully occupied axial symmetry O 2p orbitals.[4,9,128] Owing to the s orbitals being contributed to CBM, the electron transport is not affected significantly by the chemical bond direction and crystal structure randomness. That is the reason why high electron mobility occurs in ZnO and relevant materials in their polycrystalline and even amor-

phous states, and also why ZnO and relevant materials are suitable for low temperature process, such as flexible transparent electronics on polymer substrates.
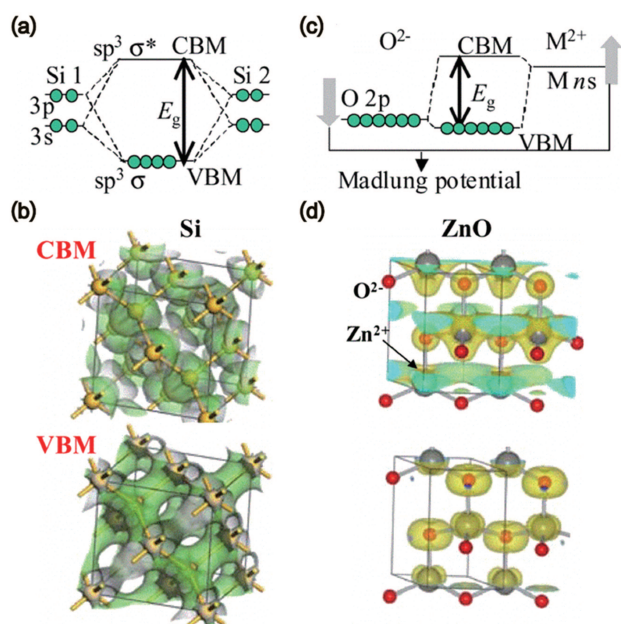

Fig. 5. (color online) Different formation mechanisms of CBM, VBM, and bandgap in silicon (a) and ZnO (c) semiconductors, as well as crystal structures and CBM/VBM wave functions in silicon (b) and ZnO (d) semiconductors.[128]

To further extend the *s* orbital of ZnO and thus to achieve higher electron mobility, indium (In) and tin (Sn) are often added into ZnO, because In^{3+} and Sn^{2+} have more broadspreading 5s orbitals than Zn^{2+}4s. Ternary alloys such as IZO[52,129] and ZTO[130,131] do show higher mobility than pure ZnO. However, due to the scarcity and toxicity, In is not suitable for the large demands in commercial applications as shown in Figs. 1(a) and 1(b) and the safety use in the healthcare or medical areas as shown in Figs. 1(c) and 1(d). Sn has been regarded as a more promising candidate for increasing the electron mobility in ZnO. At low process temperature, lots of point defects which may act as scattering centers and electron traps within the channel layer, are unavoidably induced into ZnO.[132–134] To suppress the concentration of V_O, cations, which has a stronger bonding with oxygen, such as gallium (Ga), Sn, aluminum (Al), magnesium (Mg), hafnium (Hf), zirconium (Zr), and Si have been incorporated into ZnO. Quarternary alloys, for example, InGaZnO,[2,4,135] InSnZnO,[96,136] MgSnZnO,[137] AlSnZnO,[138,139] HfInZnO,[140,141] ZrInZnO,[142] and SiInZnO,[143,144] have been reported to have improved their performances and stabilities.

As listed in Table 1, the most commonly used synthesis technique for growing ZnO channel layer on polymers is still sputtering because its simplicity and effectiveness. Another widely used technique is solution processing techniques, including spin-coating, ink-jet printing, chemical bath deposition, etc.[19,95,115] Although these synthesis technics are important and widely used, there is not much difference in the device fabrication technique between rigid and flexible substrates, and they have been described in detail in many reviews.[11,12,18,19,21,113,114] Therefore, they will not be discussed here.
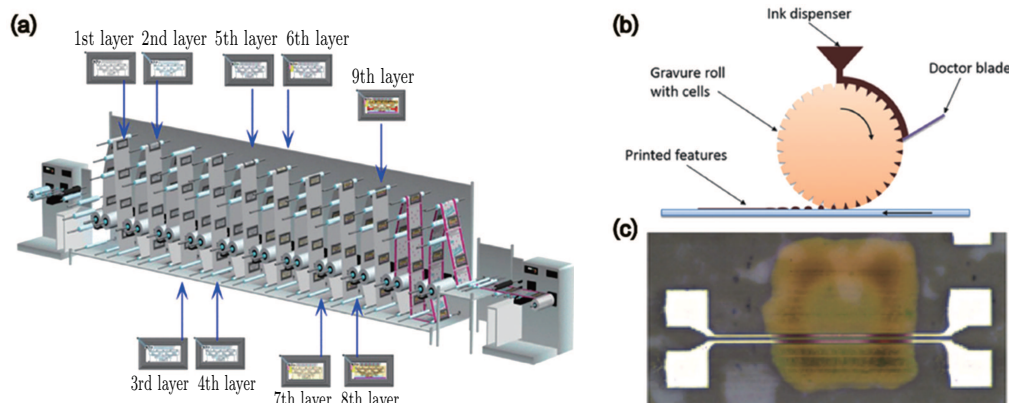

Fig. 6. (color online) Descriptive scheme for R2R/R2S gravure printing procedure. (a) R2R gravure printing system used to print RF sensor tags and smart packaging on a single line,[145] (b) overview of a gravure printing process, and (c) optical micrograph of a printed TFT.[147]

On the other hand, roll-to-roll (R2R), sheet-to-sheet (S2S), and roll-to-sheet (R2S) printing technologies hold great promise and offer advantages over classic microfabrication.[61,145] It allows extremely low manufacture cost, large fabrication area, fast printing speed on the order of meters per second,[146] and fine feature size of sub-10 μm.[147] The above-mentioned unique advantages make it a perfect candidate for applications in cheap, portable, large-volume and disposable systems, such as radio-frequency identification (RFID) tags, flexible displays, and food packaging.[148–150] Figure 6 shows the schemes of an R2R (Fig. 6(a)) and R2S (Fig. 6(b)) gravure printing system, which describes a typical flexible device fabrication procedure. In each of the R2R gravure printing units, one particular material based ink is selected to print the functional layers, i.e., buffer layers, electrodes, active layers, insulators, passivation, logos, etc. The

cells are filled with inks from an ink reservoir and wiped using a doctor blade, afterthat, the inks are transferred from the roll to the flexible substrate. Patterns are defined by recessed cells that are engraved into a roll. After the transfer process, the individual aliquots of inks spread and dry to form the final pattern. After going through each gravure printing unit, multi-functional layers are formed, patterned and aligned to each other as shown in Fig. 6(c).

2.3. Dielectric layers

As the name indicates, the transistor means transfer + resistor, which is essentially a variable resistor whose resistance is determined by the external electric field, which is generated by the gate voltage (V_g) within a metal–insulator–semiconductor (MIS) capacitor. Therefore, the quality of the bulk dielectric and interface of semiconductor/dielectrics is of the vital importance. Currently, there are three types of dielectric materials, that is, inorganic dielectric, organic dielectric, and organic dielectric/inorganic hybrid dielectric dielectric, which are commonly used in the flexible ZnO TFTs in the literature.

2.3.1. Inorganic dielectrics

Silicon dioxide (SiO_2) and silicon nitride (Si_3N_4) are two kinds of inorganic dielectric materials adopted in a-Si:H and poly-Si TFTs.[24] However, the high deposition temperature above 300 °C for high-quality film by industrialized plasma enhanced chemical vapor deposition (PECVD) hinders their application to flexible substrates. Instead of SiO_2[39] and Si_3N_4,[77] high-k dielectrics are more widely used in flexible transparent ZnO TFTs, because they can be synthesized at low temperature by atomic layer deposition (ALD)[151] or solution processes. We have deposited aluminum oxide (Al_2O_3), a typical high-k dielectric material, on rigid silicon, quartz, flexible PEN and PI substrates by ALD at low temperatures of 150 °C, 150 °C, 100 °C and 100 °C, respectively. The capacitance–voltage (C–V) measurements of ZnO/Al_2O_3/ITO MIS capacitors at a frequency of 50 kHz on different substrates are shown in Fig. 7. The Al_2O_3 insulators show comparable insulating performances on rigid quartz substrate and flexible PEN, PI substrates. The 50-nm-thick Al_2O_3 on PEN exhibits a capacitance density of 1.5×10^{-7} F/cm^2 and dielectric constant of 8.47, which is basically equivalent to the dielectric property of the Al_2O_3 film fabricated on quartz.
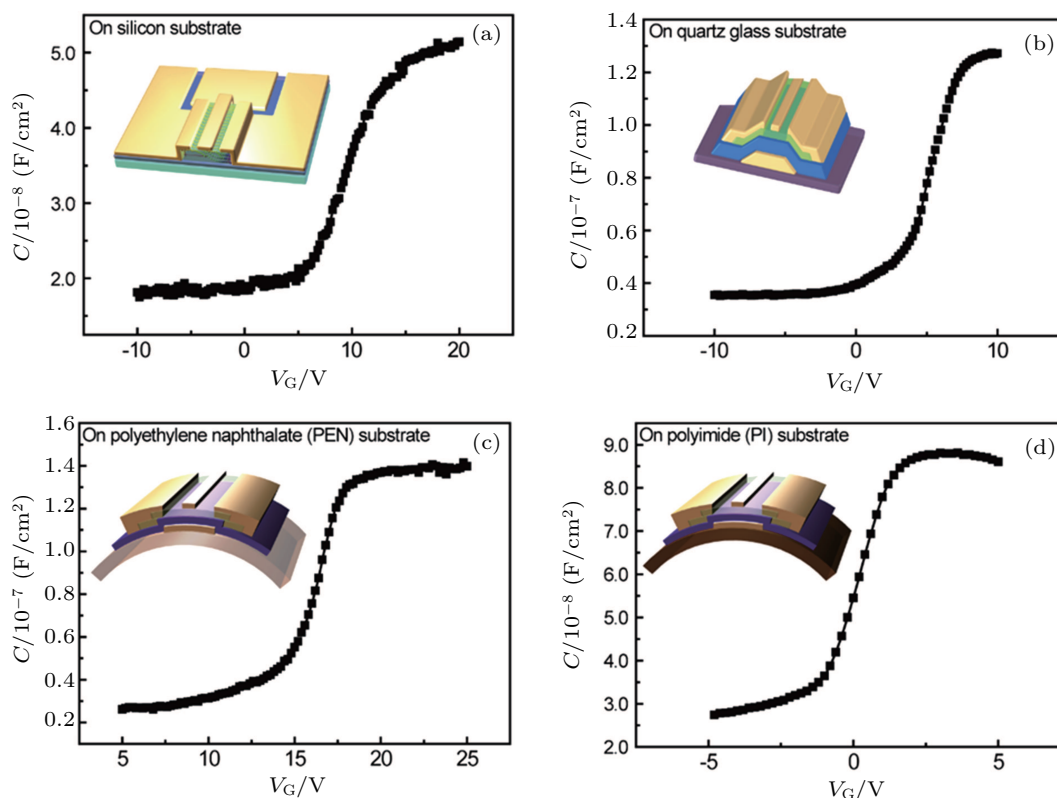

Fig. 7. (color online) Capacitance–voltage (C–V) measurements of Al_2O_3 dielectrics deposited at low temperatures on (a) p^{++}-silicon, (b) quartz glass, (c) PEN, and (d) PI substrates.

2.3.2. Organic dielectrics

Inorganic dielectric, such as Al_2O_3, has exhibited low-temperature fabrication convenience and excellent device performance. However, mechanical failure may occur when the film is under tensile or compressive strain as shown in Fig. 8. Jen *et al*. reported that a 80-nm-thick ALD-grown Al_2O_3 film could only sustain a strain level of 0.52%.[152] Xu *et al*. claimed the critical strain, a critical point at which the film be-

comes useless, for 200-nm-thick anodized Al_2O_3 film on PEN is 0.6%.[66] If the thickness of the flexible substrate is 125 μm, the critical bending radius is approximately 10 mm (See Section 3 for more details of mechanical bending), which is not suitable for some flexible, foldable or stretchable applications.
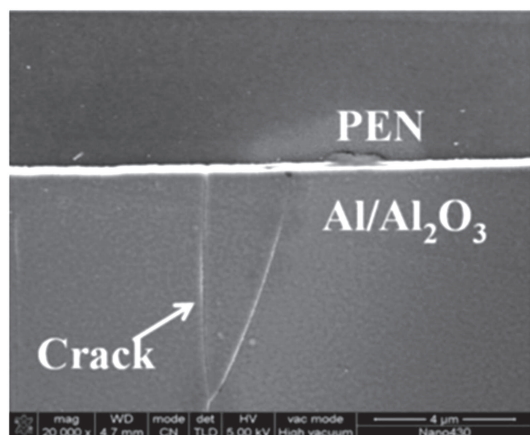

Fig. 8. FESEM image of cracks in Al_2O_3 film with a thickness of 200 nm on PEN after 0.6% strain.[66]

Nevertheless, organic dielectric materials,[153] such as poly(4-vinylphenol) (PVP), poly(methyl methacrylate) (PMMA) and polystyrene (PS), can sustain larger strain[91] because the molecules in them are linked through van der Waals bond and/or hydrogen bond, and they are weakly interacting. In addition, polymer dielectrics can be formed by simple and low-cost processes, such as spin-coating and printing. The characteristics of these materials can be tuned by designing the molecular precursors and polymerization reaction conditions, which offer more application opportunities in a wide range of electronic devices. Figure 9 shows the chemical structures of typical polymeric gate dielectrics.
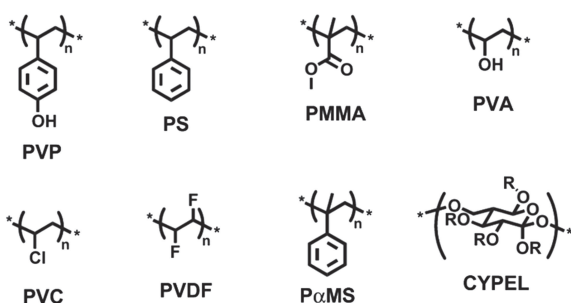

Fig. 9. Chemical structures of some typical polymeric dielectrics.[154]

Lai *et al.* fabricated ultra-flexible IGZO TFT on 125-μm-thick PET substrate with PVP used as polymeric gate dielectrics, on which device performance shows no degradation upon bending to strain $\varepsilon = 1.5\%$.[43] Kim *et al.* also reported flexible IGZO TFT on PET substrate with PMMA as gate dielectrics.[155] However, they did not perform the bending test evaluation. Up to now, the reports of flexible transparent ZnO TFTs with pristine polymeric gate dielectrics have been still quite limited.

The stable and efficient operation of flexible transparent ZnO TFTs under mechanical stress requires all of the components to work stably and reliably. Lai *et al.* proposed that the polymeric gate dielectrics can also reduce the stress in the IGZO channel layer.[43] The Young's modulus for polymer material is around several GPa. However, it is more than 100 GPa for oxide based inorganic semiconductor. This large difference enables the stress to be mainly located at the polymer side, leaving the IGZO layer less stressed as shown in Fig. 10.
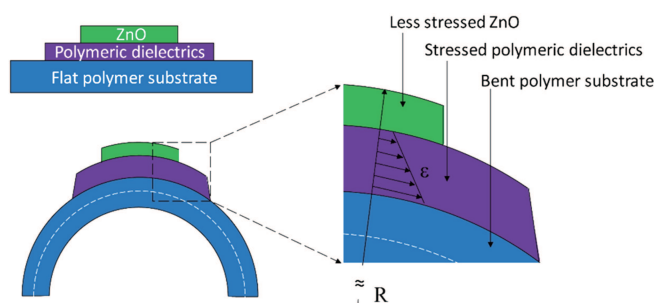

Fig. 10. (color online) The schematic descriptions of the stacked ZnO/polymeric dielectrics/polymer structure in flat and bent states, respectively. In the bent state, the stress is mainly located within the polymeric dielectrics layer.

2.3.3. Organic/inorganic hybrid dielectrics

Although polymeric dielectrics sustain greater strain than their inorganic counterparts and can relax the stress in the channel layer, they have some drawbacks as follows.

i) Polymers are usually soft, and thus deposition of channel layer may induce damages inside polymer layer or at the polymer/channel interface, which will significantly influence the transport behaviors of field-modulated electrons.

ii) The values of dielectric constant (k) of most polymers are relatively low ($\varepsilon_r = 2.5$–2.6 for PVP), which would exhibit smaller capacitance at a given thickness than inorganic dielectric materials.

iii) The polymeric dielectrics are more hydrophobic than inorganic materials, which is undesirable for directly growing the channel semiconductors.

Besides utilizing stacked organic/inorganic hybrid dielectric gate,[156] these problems could also be solved by introducing inorganic nanoparticles into polymer matrices to form polymer nanocomposites. Lai *et al.* fabricated a nanocomposite dielectrics by incorporating high-k Al_2O_3 nanoparticles into polymer PVP films as shown in Fig. 11.[68] Al_2O_3 nanoparticles (size < 50 nm) was added into PVP/poly(melamine-co-formaldehyde) precursor at a concentration in a range from 0.25 wt% to 1.00 wt%. After being stirred overnight, the solution was spin-coated on silver (Ag) gate. The nanocomposite dielectric was then post-treated with hot plate and ultraviolet illumination. The capacitance of the pristine PVP was 14 nF/cm^2 corresponding to a dielectric constant of 3.9. After adding 0.25, 0.5-wt% and 1-wt% Al_2O_3 nanoparticles, the capacitance increased to 19,

20, and 22 nF/cm^2, and the corresponding dielectric constants increased to 6.1, 7.1, and 8.1. After that, the lead oxide (PbO), which is a high-k material with $\varepsilon_r = 200$,[157] was introduced into PVP polymer, and the dielectric constant increased to 21.2.[158] Along with the improved capacitance, the TFT with nanocomposite dielectrics could sustain the same strain as the device with pristine PVP dielectrics.[43,68] This means that the nanocomposite dielectric inherits the merits from both inorganic high-k material and organic polymer material. In addition, the incorporation of high-k nanoparticles into polymeric dielectrics was believed to improve the robustness against the plasma damage in the following sputtering process.[68] In general, organic materials are more hydrophobic than inorganic materials, which is undesirable for the direct growing inorganic semiconductor materials on the polymeric dielectrics.[159,160] However, few researchers havefocused the effects of incorporated nanoparticles on the surface energy of nanocomposite dielectric.
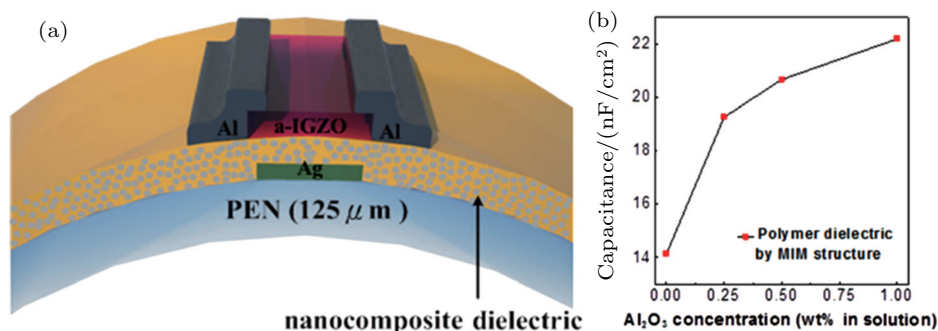

Fig. 11. (color online) Organic/inorganic hybrid nanocomposite dielectrics. (a) Schematic diagram of IGZO TFT with nanocomposite dielectrics. (b) Capacitance of nanocomposite dielectrics, which increases with Al$_2$O$_3$ concentration increasing.[68]

2.4. Electrode layers

The gate and source/drain electrodes in flexible transparent ZnO TFTs should possess at least three characteristics: low conductive resistivity, high optical transmittance, and good mechanical stability. Yet the most widely used flexible transparent electrodes (FTEs) are transparent conductive oxides (TCOs), represented by ITO, FTO, AZO, GZO, IZO, ZTO, and IZTO, as they have wide bandgaps, low resistivities and can be deposited at low temperatures.[161,162] However, the mechanical stability of TCO electrode is still a tough issue to be solved for achieving stable and reliable device operation.[163–166]

Leterrier *et al.* investigated the effect of ITO thickness on the crack onset strain (COS), the critical strain at failure of the film.[163] The evolution of film mechanical failure under uniaxial strain was recorded as shown in Fig. 12 as growing ITO film has some microdefects in the form of pin-holes (Fig. 12(a)). Upon reaching a strain of 1.28%, small cracks originating from the microdefects appeared (Fig. 12(b)). Further increasing the strain to 1.42%, the initial crack propagated from the sites to finite size (Fig. 12(c)) and the resistivity began to increase as shown in the onset region in Fig. 12(e). At higher strain levels, the finite cracks increased and the width spanned to the whole sample (Fig. 12(d)). As a result, the resistivity increased markedly as can be seen in Fig. 12(e). They found that the COS decreased with ITO thickness, which means that for a thicker ITO film the safe operating range could be even smaller.
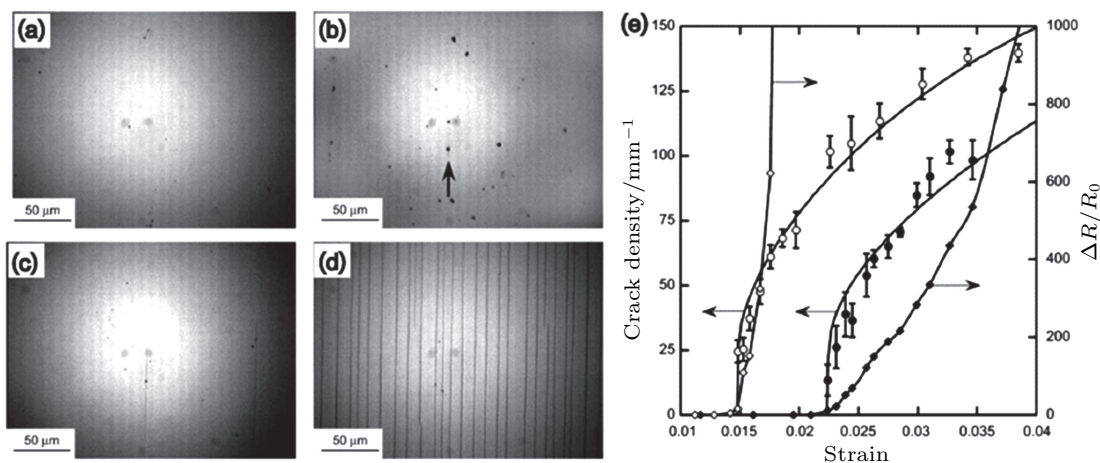

Fig. 12. Progressive cracking of a 100-nm thick ITO film on 100-μm thick polyester substrate during tensile loading (along the horizontal direction). Unloaded ITO (a); at 1.28% strain (b), the arrow indicates the failure initiation on a coating defect); at 1.42% strain (c); and at 3.42% strain (d). Density of tensile cracks and normalized resistance change during tensile loading of 50 nm (solid symbols) and 100 nm (empty symbols) thick ITO (e).[163]

To seek for flexible transparent electrodes which can sustain higher mechanical strains, oxide–metal–oxide (OMO) stacked structure (Fig. 13(a)) has been proposed. The most commonly used metal materials are silver (Ag) and copper (Cu) because of their good ductilities and high conductivities. What is more, by optimizing the metal layer thickness, the figure of merit (FOM), which can comprehensively characterize the property of transparent electrode, can be improved.[167] By inseting a thin Ag layer into the middle of double 30-nm-thick IZO layers,[168–171] the IZO/Ag/IZO stacked electrode showed improved optical transmittance and conductive resistivity (Fig. 13(b)).[171] Maximum improvement of FOM was obtained with a 12-nm-thick Ag layer (Fig. 13(c)). More importantly, the mechanical robustness was improved compared with a single ITO layer (Fig. 13(d)). Other reported stacked electrodes with improved electrical conductivity, optical transmittance and mechanical robustness involve ITO/Ag/ITO,[172,173] IZTO/Ag/IZTO,[174] GZO/Ag/GZO,[175] IZO/Ag/IZO, ZTO/Ag/ZTO,[176,177] IZO/Ag/IZO/Ag,[170] and ITO/Cu/ITO.[173]
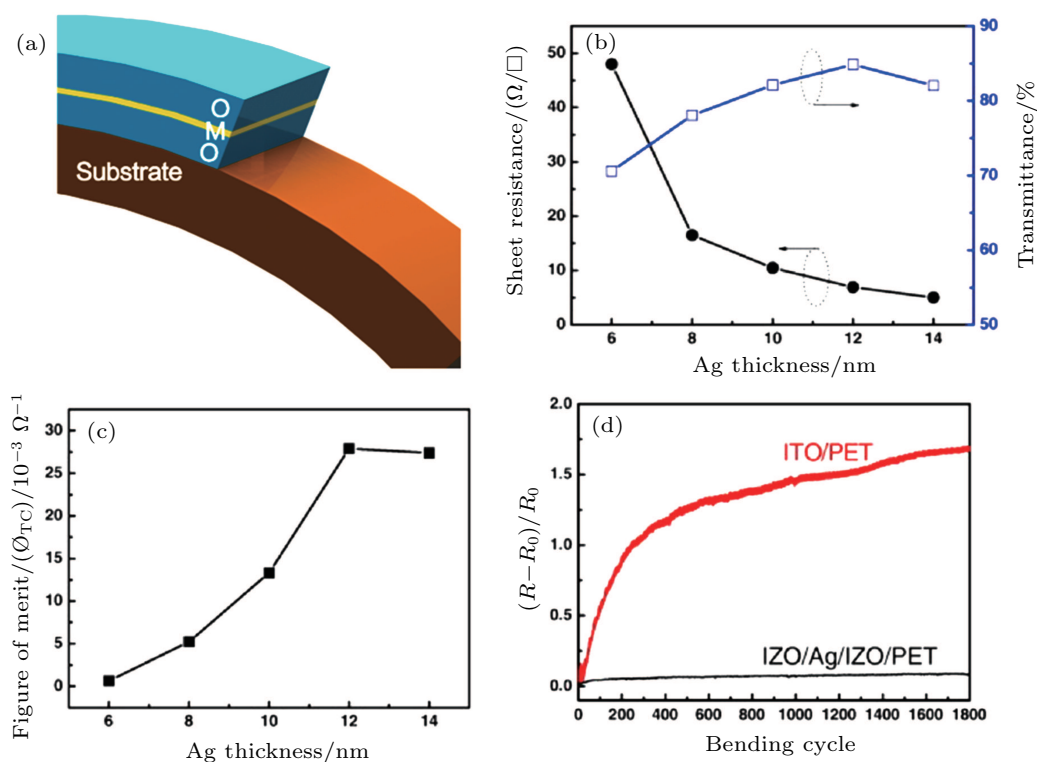

Fig. 13. (color online) OMO stacked electrode. (a) Schematic diagram of a typical OMO stacked electrode. (b) Sheet resistance, transmittance at 550 nm. (c) FOM of an IZO/Ag/IZO multilayer anodes on PET substrates as a function of the Ag thickness. (d) Normalized resistance change after repeatedly bending as a function of the number of cycles for IZO/Ag/IZO/PET and amorphous ITO/PET sample.[171]
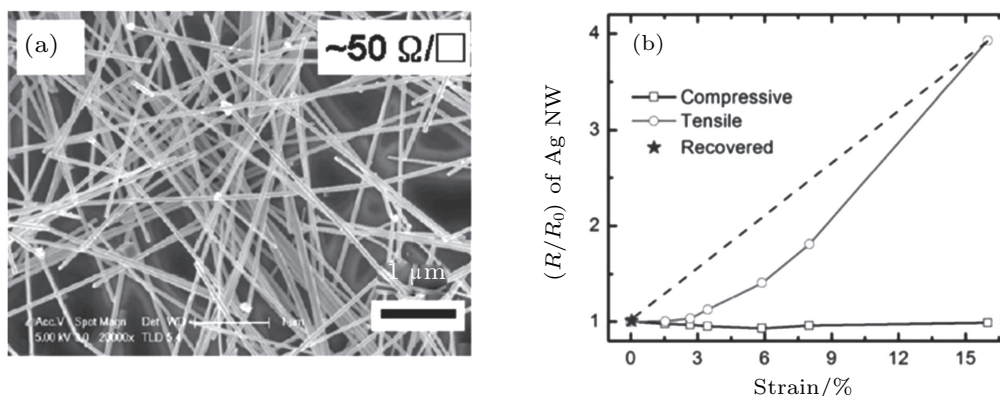

Fig. 14. Random meshed Ag NW electrode. (a) SEM image of Ag NWs on flexible transparent substrate.[182] (b) Surface resistance ratio (R/R_0) of the Ag NW/polymer electrode comparing tensile and compressive strains.[179]

The random meshed Ag nanowire (Ag NW)[178–182] electrode is another promising candidate for flexible transparent ZnO TFTs, as Ag forms ohmic contact with ZnO.[104] The unique advantage of Ag nanowire electrodes is their mechanical robustness, because nano-materials can be bent to much smaller radii than conventional "3D" materials.[183] Figure 14(a) shows the SEM image of random meshed Ag NWs on a flexible substrate[182] and figure 14(b) shows the resis-

tance change as a function of mechanical strains.[179] Compared with the small COS of ITO shown in Fig. 12, the Ag NW flexible transparent electrode processes much better mechanical robustness, with only 3.9 times increase of resistance under 15% tensile strain and almost no change under 15% compressive strain.

3. Bending effect on flexible TFT

Operation of flexible transparent ZnO TFTs often involves the mechanical deforming of substrate, so the understanding of the evolution of device performance under stress is of fundamental importance for conducting the research in this area.[184,185] In fact, the requirements for flexibilities of devices are quite different when they are used in different areas. In the case of flexible display, the device may need a large strain tolerance when it was rolled up like a scroll.[6] In skin sensors and wearable electronics, devices may go through small but repeated strains.[22] Despite the differences, the mechanical processes all follow the same basic principles. So in this section, we will review the mechanical fundamentals on flexible transparent ZnO TFTs and focus on the test technique, strain calculation and characterization methods. Finally, the present reports on flexibility test of ZnO TFTs will be briefly depicted.

3.1. Bending test systems

The bending test systems reported in the literature are all laboratory-made and can be roughly classified as two types according to how devices are bent: 1) substrate wrapped around a rigid rod (Fig. 15(a)) and 2) arched up under side extrusion (Fig. 15(b)). In type 1, the probe tips contact well with the electrodes. However, the variation of bending radius is not convenient in this setup. On the contrary, in type 2, the bending radius can be tuned by varying the distance between the two splints. But the probe tips might contact poorly with the electrodes especially when the substrate is thin or soft.[88] Thus, attaching flexible polymer substrate onto a flexible metal sheet might be a good choice to combine good contact and flexibility.
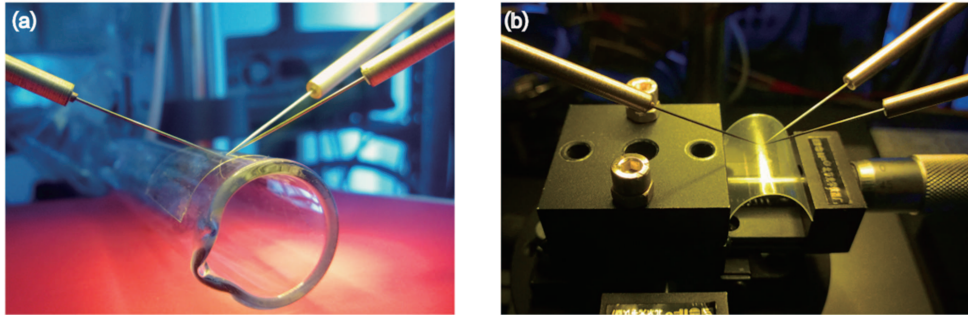

Fig. 15. (color online) Two types of bending test systems. (a) Substrate wrapped around a rigid rod and (b) arched up under side extrusion.

3.2. Strain in film

In a simplified case (no Poisson ratio nor fabrication-induced strain), the strain (ε) within the film on bending substrate can be roughly obtained through Eq. (1), under the premise that the substrate is much thicker than the film, or Eq. (2), under the assumption of neglecting the difference in Young's modulus between substrate (Y_s) and film (Y_f). Both the two mechanical models simplified the calculation process and were suited well for many other cases.[43,68,186]

$$\varepsilon = \frac{d_s}{2R},\tag{1}$$

$$\varepsilon = \frac{d_s + d_f}{2R},\tag{2}$$

where d_s is the thickness of substrate, d_f the thickness of film, and R the bending radius.

For the case in which neither the premise nor the assumption holds, one could go to Eq. (3)[187–189]

$$\varepsilon = \left(\frac{d_s + d_f}{2R}\right)\frac{(1 + 2\eta + \chi\eta^2)}{(1 + \eta)(1 + \chi\eta)},\tag{3}$$

where $\eta = d_f/d_s$ and $\chi = Y_f/Y_s$.

The relationships between ε and d_s, R, η, χ in Eq. (1) and Eq. (3), are visualized in Figs. 16(a) and 16(b) (setting $d_s = 100$ μm and $R = 5$ mm). As can be seen in Fig. 16(a), at a fixed radius, the strain can be reduced by utilizing a thin substrate. At a fixed d_s, the strain increases markedly with radius decreasing, and the critical failure radius increases with d_s increasing. Taking d_f and the difference between Y_f and Y_s into account, the strain could become smaller with η and χ increasing as can be seen in Fig. 16(b).

For a given film (fixed d_f and Y_f), besides using thinner and more elastic substrates described above, there are other ways to reduce the strains in functional films. By encapsulating the film and forming an encapsulation/film/substrate sandwiched structure, the strains in film can be further reduced.[189] If the configuration meets

$$Y_s d_s^2 = Y_e d_e^2,\tag{4}$$

where Y_e and d_e are the Young's modulus and thickness of the encapsulation layer, respectively, the film without any strain

is right in the neutral surface. Consequently, the functional film will not fail to work until the substrate and encapsulation are ineffective. In this approach, Sekitani *et al.* fabricated ultra-flexible organic TFT with a sandwiched poly-chloro-paraxylylene/pentacene-TFT/PI structure[190] and Kinkeldei *et al.* reported sandwiched PI/IGZO TFT/PI structure with a small bending radius of 125 μm.[40] Park *et al.* proposed that inserting a buffer layer between film and substrate can also reduce the film strain.[191]
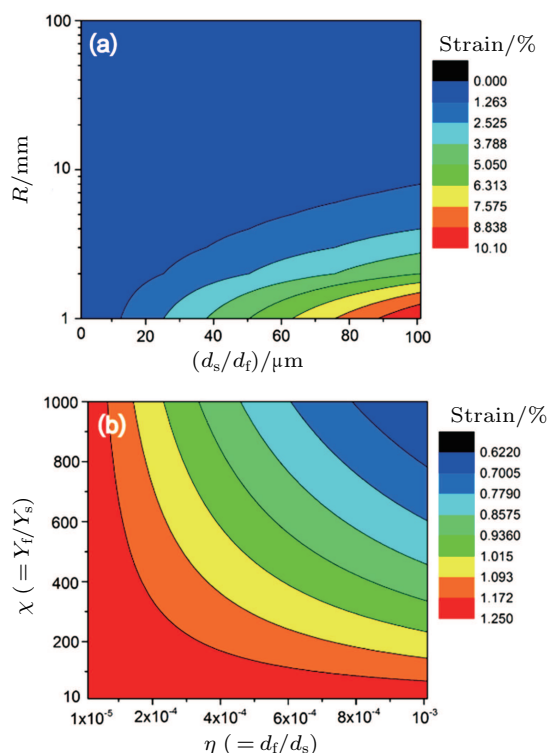

Fig. 16. (color online) Visualizations of relationships (a) between R and $(d_s + d_f)$ and (b) between χ and η.

3.3. Bending direction

In practical applications, the flexible transparent ZnO TFTs might be bent into various forms, and thus the functional films would sustain various kinds of strains, such as tensile, compressive and twisting. Besides conventional electrical field, the mechanical stress field is also an important issue that must be included in the analysis of flexible electronics. For flexible IGZO TFT, the tensile strains parallel (Fig. 17(a)) and perpendicular (Fig. 17(b)) to the current flow have different effects on electrical performance.[42] As shown in Fig. 17(c), saturation mobility (μ_{sat}) is slightly affected by the strain parallel to the channel up to $\varepsilon = 0.72\%$, while μ_{sat} begins to be degraded when $\varepsilon > 0.3\%$ under a strain perpendicular to channel. The degradations of both on- and off- currents of flexible TFT under the perpendicular strain are explained as being due to the crack of brittle chromium (Cr) gate. The cracks disconnect the parts of gate, leaving some of the channel areas uncontrolled, thus making the off-current increased and the on-current reduced. Whereas, no crack occurs under the parallel

strain when $\varepsilon < 0.72\%$. Once ε exceeds 0.72%, the cracks become unstable and destroy the device permanently.
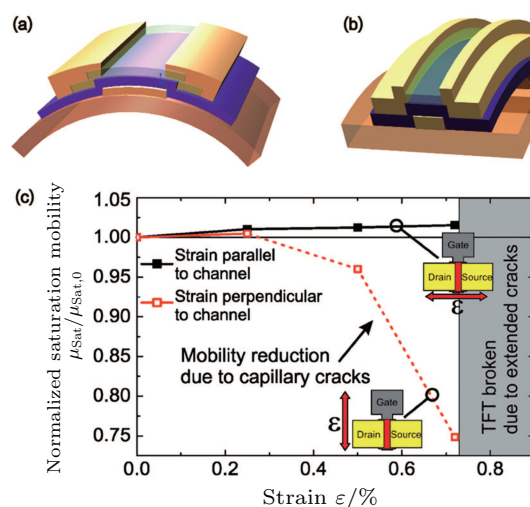

Fig. 17. (color online) Strain directions with respect to the channel direction. Schematic of tensile strains (a) parallel and (b) perpendicular to the channel direction in flexible TFT. (c) Normalized IGZO saturation mobility changes induced by mechanical strains parallel or perpendicular to channel.[42]
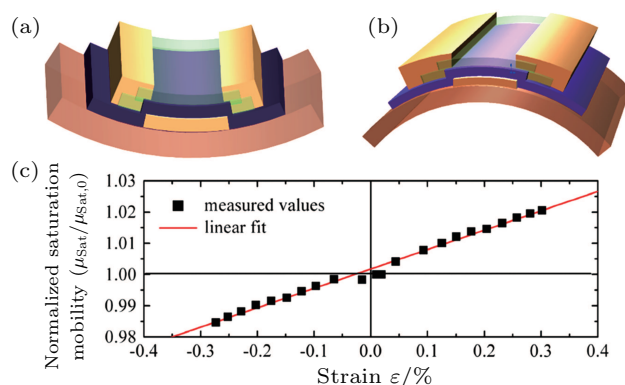

Fig. 18. (color online) Strain types under inward or outward bending. Schematic description of (a) tensile and (b) compressive strains in flexible TFT. (c) Normalized IGZO TFT linear mobility varying with compressive and tensile strains.[194]

Bending the TFTs outwards causes a tensile strain, while bending the TFTs inwards causes a compressive strain. Compared with the tensile strain, the compressive strain has a relatively small effect on the electrical performance.[192–194] The influence of strain on the electron transport mobility can be described as follows:

$$\frac{\mu_{bent}}{\mu_0} = 1 + m\varepsilon, \tag{5}$$

where μ_0 and μ_{bent} are the charge carrier mobilities respectively in flat and bent conditions, and *m* is an empirical proportionality constant which depends on the channel material.[195] For IGZO, Petti *et al.*[72] and Münzenrieder *et al.*[194] found that the tensile and compressive strains could induce TFT parameters shifting towards opposite directions as shown in Fig. 18. Under a tensile strain, the field mobility and subthreshold swing are increased, and the threshold voltage is reduced; while under a compressive strain, the field mobility

and subthreshold swing are reduced, and the threshold voltage is increased. The dependence of electrical performance on the strain types can be explained with the electrical structure change associated with crystal structure deformation.[85,196]

3.4. Reports on strain test

The maximum operation strain of flexible transparent ZnO TFT depends on the mechanical property of each of the functional layers. Devices with high robustness that can sustain high intense and repeated bending are always desirable. In Table 3 summarized is the state-of-art results about bending test of flexible transparent ZnO TFTs. Most of the polymer substrates listed in Table 3 are PI, PET, and PEN with thickness values ranging from 1 to several hundred microns. For either wrapped around rigid rods or arched up with two paral-

lel plates, majority of the devices are bent with tensile strain parallel to the current flow (channel length direction). However, compressive strain or strain perpendicular to current flow should also been considered since they could have different influences on the flexible ZnO TFT performance.[42,194] Generally, smaller bending radii are desirable, because it means more flexibilities and serviceabilities. Bending radius can vary in a large range from 25 μm to 10 cm depending mainly on the thickness of the substrate. Strain is in inverse proportion to bending radius as shown in Eqs. (1)–(3), and is the normalized parameter to describe the mechanical state in functional layer whatever the substrate thickness is. Fatigue test concerns the stability and reliability of flexible device. Typically, the fatigue tests conduct 10^2 to 10^6 times with respect to the stressing times.

Table 3. Results of bending test of flexible transparent ZnO TFTs in the period from 2010 to 2016.

Substrate	Setup	Paral. or perp. to current flow	Compressive or tension	Bending degree		Bending times	Ref.	Year
				Radius/mm	Strain/%			
50-μm PI	arch	–	tensile	10/5	0.56/1.06	–	Cherenack et al.[26]	2010
220-μm PET	–	paral.	–	40	0.28	–	Liu et al.[35]	2010
50-μm PI	arch	–	tensile	0.25	6.35	100	Song et al.[29]	2010
50-μm PI	arch	paral.	compressive	0.125	–	–	Kinkeldei et al.[40]	2011
50-μm PI	wrap	both	tensile	3.5	0.72	20000	Münzenrieder et al.[42]	2012
125-μm PEN	wrap	–	–	4	1.5	100	Lai et al.[43]	2012
125-μm PI	–	–	tensile	5	1.25	–	Kim et al.[45]	2012
50-μm PI	wrap	paral.	tensile	7	0.36	–	Yang et al.[51]	2013
50-μm PI	wrap	paral.	tensile	3.5	0.72	–	Münzenrieder et al.[58]	2013
50-μm PI	wrap	paral.	tensile	3.5	0.72	–	Münzenrieder et al.[59]	2013
50-μm PI	wrap	paral.	tensile	5	0.5	–	Zysset et al.[60]	2013
PET	arch	–	both	4	–	6	Ji et al.[47]	2013
PET	–	–	–	20	–	–	Zhou et al.[52]	2013
50-μm PI	–	–	tensile	5	1	10000	Hong et al.[49]	2013
100-μm glass	–	perp.	–	70	–	100	Dai et al.[62]	2013
200-μm PET	arch	–	both	-4.2/4.3	–	10000	Kim et al.[48]	2013
50-μm PEN	arch	–	both	4	0.6	10^6	Xu et al.[66]	2014
120-μm PI	–	–	–	10	–	–	Wee et al.[64]	2014
125-μm PEN	wrap	perp.	tensile	4	1.56	100	Lai et al.[68]	2014
PES	–	–	both	18	0.55	–	Park et al.[63]	2014
1-μm parylene	wrap	paral.	tensile	0.05	0.4	–	Salvatore et al.[23]	2014
70-μm glass	wrap	perp.	tensile	40	0.09	–	Lee et al.[74]	2014
50-μm PI	wrap	paral.	tensile	4	0.4	–	Münzenrieder et al.[73]	2014
1-μm PI	wrap	both	compressive	0.025	–	–	Karnaushenko et al.[16]	2015
PC	–	–	–	20	–	100	Hsu et al.[86]	2015
10-μm PI	–	–	tensile	2.6	–	1000	Honda et al.[78]	2015
5-μm PI	wrap	paral.	tensile	3.5	0.07	50000	Li et al.[75]	2015
PET	wrap	paral.	tensile	10	–	1000	Liu et al.[76]	2015
25-μm PEN	–	both	tensile	2	0.75	4000	Tripathi et al.[85]	2015
125-μm PEN	arch	paral.	tensile	3.3	1.9	10000	Park et al.[83]	2015
50-μm PI	wrap	perp.	tensile	5	0.48	–	Petti et al.[84]	2015
17-μm PI	arch	both	tensile	1.5	3.5	10000	Park et al.[91]	2016
3-μm PI	wrap	–	tensile	0.15	–	–	Kim et al.[93]	2016
200-μm PES	both	paral.	tensile	12	0.8	2000	Oh et al.[94]	2016
500-μm PDMS	wrap	–	tensile	15	–	–	Jung et al.[92]	2016
20-μm PI	wrap	–	tensile	100	–	–	Zhang et al.[89]	2016
125-μm PEN	arch	paral.	tensile	8	0.78	–	Zhang et al.[88]	2016

4. Conclusions and perspectives

The flexible and transparent electronics has received particular attention in electronic material, device and circuit areas, especially in the last thirteen years. Mechanical deformation capability, light weight, low cost and other unique advantages make it better than conventional electronic circuits which are based on rigid substrates, like silicon and glass. The inorganic flexible transparent electronic devices and products are mainly based on ZnO and relevant materials, owing to their high electrical properties, good optical transparency and low-synthesis temperature. On the contrary, the requirement for uniform material growth in large area at low-temperature rules out other inorganic semiconductors, such as Si, GaN, and SiC, which needs elevated temperatures for good material quality. In this paper, we give a brief introduction of recent advances in flexible transparent TFTs based on ZnO and relevant materials, and discuss several important issues of device physics and fabrication technology relating to the substrate, electrodes, channel and dielectric layer in Section 2. The operation and evaluation of strain test are highlighted in Section 3.

The advent of flexible transparent electronics has also boosted the development of solution process techniques, especially roll-to-roll printing and other printing technics.[19,21,115,162,181] The inks used in printing techniques will need to dissolve the zinc precursors into solvents, such as dissolving zinc hydroxide ($Zn(OH)_2$) into aqueous ammonia (NH_4OH),[37,49] zinc acetate dihydrate [$Zn(CH_3COO)_2$] into 2-methoxyethanol ($CH_3OCH_2CH_2OH$)[28,46,93,95,197–200] and zinc chloride ($ZnCl_2$) into ethylene glycol ($C_2H_6O_2$).[62] Thus, a high-temperature (> 300 °C) post-annealing is essential to fully decompose the organic components and produce a pure-phase metal oxide from the solution phase, which is not compatible with most of the flexible substrates.[49] To solve this problem, some low-temperature post-treatment is conducted on solution processed ZnO TFTs, including microwave annealing[37,197–199,201] and ultraviolet photo annealing.[46,202,203] However, most of the researches are based on rigid silicon or glass substrates, very limited reports on flexible substrates.[63] So, we suggest that low-temperature post-treatment can be a promising direction for solution processing, especially printing, techniques. The flexibility also involves mechanical stability issue, which never presents in traditional rigid devices. The strain in the film will induce mechanical stress field which can change the crystal, and thus electrical, structure and even crack the oxide films.[204] Critical parameters such as energy band, mobility, dielectricity, and thermal conductivity can also be affected. Thus, coupling of multi-physics involving mechanical stress field needs to be rigorously studied. Finally, the commercialized application still requires the long-term stable, repeatable, reliable, large-area uniform, and t low cost techniques.

Despite the problems that are to be solved, due to the rapid development, we have plenty of reasons to keep optimistic for the coming era of flexible transparent technology.

References

[1] Hoffman R L, Norris B J and Wager J F 2003 *Appl. Phys. Lett.* **82** 733
[2] Nomura K, Ohta H, Ueda K, Kamiya T, Hirano M and Hosono H 2003 *Science* **300** 1269
[3] Wager J F 2003 *Science* **300** 1245
[4] Nomura K, Ohta H, Takagi A, Kamiya T, Hirano M and Hosono H 2004 *Nature* **432** 488
[5] Carcia P F, McLean R S, Reilly M H and Nunes G Jr 2003 *Appl. Phys. Lett.* **82** 1117
[6] Park J S, Kim T W, Stryakhilev D, Lee J S, An S G, Pyo Y S, Lee D B, Mo Y G, Jin D U and Chung H K 2009 *Appl. Phys. Lett.* **95** 13503
[7] Tripathi A K, Smits E C P, van der Putten J B P H, van Neer M, Myny K, Nag M, Steudel S, Vicca P, O'Neill K, van Veenendaal E, Genoe J, Heremans P and Gelinck G H 2011 *Appl. Phys. Lett.* **98** 162102
[8] Reyes P I, Ku C J, Duan Z, Lu Y, Solanki A and Lee K B 2011 *Appl. Phys. Lett.* **98** 173702
[9] Kamiya T and Hosono H 2010 *Npg Asia Mater.* **2** 15
[10] Dagdeviren C, Hwang S W, Su Y, Kim S, Cheng H, Gur O, Haney R, Omenetto F G, Huang Y and Rogers J A 2013 *Small* **9** 3398
[11] Fortunato E, Barquinha P and Martins R 2012 *Adv. Mater.* **24** 2945
[12] Petti L, Münzenrieder N, Vogt C, Faber H, Büthe L, Cantarella G, Bottacchi F, Anthopoulos T D and Tröster G 2016 *Appl. Phys. Rev.* **3** 21303
[13] Cherenack K, Zysset C, Kinkeldei T, Münzenrieder N and Tröster G 2010 *Adv. Mater.* **22** 5178
[14] Lee S, Jeon S, Chaji R and Nathan A 2015 *Proc. IEEE* **103** 644
[15] Makarov D, Melzer M, Karnaushenko D and Schmidt O G 2016 *Appl. Phys. Rev.* **3** 11101
[16] Karnaushenko D, Münzenrieder N, Karnaushenko D D, Koch B, Meyer A K, Baunack S, Petti L, Tröster G, Makarov D and Schmidt O G 2015 *Adv. Mater.* **27** 6797
[17] Münzenrieder N, Cantarella G, Vogt C, Petti L, Büthe L, Salvatore G A, Fang Y, Andri R, Lam Y, Libanori R, Widner D, Studart A R and Tröster G 2015 *Adv. Electron. Mater.* **1** 1400038
[18] Kwon J Y, Lee D J and Kim K B 2011 *Electron. Mater. Lett.* **7** 1
[19] Ahn B D, Jeon H J, Sheng J, Park J and Park J S 2015 *Semicond. Sci. Technol.* **30** 64001
[20] Mativenga M, Geng D, Kim B and Jang J 2015 *ACS Appl. Mater. Interfaces* **7** 1578
[21] Kim S J, Yoon S and Kim H J 2014 *Jpn. J. Appl. Phys.* **53** 02BA02
[22] Romeo A and Lacour SP 2015 37th Annual International Conference of the IEEE Engineering in Medicine and Biology Society (EMBC), August 25–29, 2015, Milano, Italy, p. 8014
[23] Salvatore G A, Münzenrieder N, Kinkeldei T, Petti L, Zysset C, Strebel I, Büthe L and Tröster G 2014 *Nat. Commun.* **5** 2982
[24] Kagan C R and Andry P 2003 *Thin-Film Transistors*, 2nd edn. (New York: CRC Press) pp. 55–61
[25] Fleischhaker F, Wloka V and Hennig I 2010 *J. Mater. Chem.* **20** 6622
[26] Cherenack K H, Munzenrieder N S and Troster G 2010 *IEEE Electron Dev. Lett.* **31** 1254
[27] Park K, Lee D K, Kim B S, Jeon H, Lee N E, Whang D, Lee H J, Kim Y J and Ahn J H 2010 *Adv. Funct. Mater.* **20** 3577
[28] Lee C Y, Lin M Y, Wu W H, Wang J Y, Chou Y, Su W F, Chen Y F and Lin C F 2010 *Semicond. Sci. Technol.* **25** 105008
[29] Song K, Noh J, Jun T, Jung Y, Kang H Y and Moon J 2010 *Adv. Mater.* **22** 4308
[30] Zhao D, Mourey D A and Jackson T N 2010 *IEEE Electron Dev. Lett.* **31** 323
[31] Kim D H, Cho N G, Kim H G and Kim I D 2010 *Electrochem. Solid-State Lett.* **13** H370
[32] Nomura K, Aoki T, Nakamura K, Kamiya T, Nakanishi T, Hasegawa T, Kimura M, Kawase T, Hirano M and Hosono H 2010 *Appl. Phys. Lett.* **96** 263509
[33] Su N C, Wang S J, Huang C C, Chen Y H, Huang H Y, Chiang C K and Chin A 2010 *IEEE Electron Dev. Lett.* **31** 680
[34] Liu J, Buchholz D B, Hennek J W, Chang R P H, Facchetti A and Marks T J 2010 *J. Am. Chem. Soc.* **132** 11934

[35] Liu J, Buchholz D B, Chang R P H, Facchetti A and Marks T J 2010 *Adv. Mater.* **22** 2333

[36] Cheong W S, Bak J Y and Kim H S 2010 *Jpn. J. Appl. Phys.* **49** 05EB10

[37] Jun T, Song K, Jeong Y, Woo K, Kim D, Bae C and Moon J 2011 *J. Mater. Chem.* **21** 1102

[38] Jung Y, Jun T, Kim A, Song K, Yeo T H and Moon J 2011 *J. Mater. Chem.* **21** 11879

[39] Mativenga M, Choi M H, Choi J W and Jang J 2011 *IEEE Electron Dev. Lett.* **32** 170

[40] Kinkeldei T, Munzenrieder N, Zysset C, Cherenack K and Tröster G 2011 *IEEE Electron Dev. Lett.* **32** 1743

[41] Marrs M A, Moyer C D, Bawolek E J, Cordova R J, Trujillo J, Raupp G B and Vogt B D 2011 *IEEE Trans. Electron Dev.* **58** 3428

[42] Munzenrieder N, Zysset C, Kinkeldei T and Troster G 2012 *IEEE Trans. Electron Dev.* **59** 2153

[43] Lai H C, Tzeng B J, Pei Z, Chen C M and Huang C J 2012 *SID Symp. Dig. Tech. Pap.* **43** 764

[44] Erb R M, Cherenack K H, Stahel R E, Libanori R, Kinkeldei T, Münzenrieder N, Tröster G and Studart A R 2012 *ACS Appl. Mater. Interfaces* **4** 2860

[45] Kim D I, Hwang B U, Park J S, Jeon H S, Bae B S, Lee H J and Lee N E 2012 *Org. Electron.* **13** 2401

[46] Kim Y H, Heo J S, Kim T H, Park S, Yoon M H, Kim J, Oh M S, Yi G R, Noh Y Y and Park S K 2012 *Nature* **489** 128

[47] Ji L W, Wu C Z, Fang T H, Hsiao Y J, Meen T H, Water W, Chiu Z W and Lam K T 2013 *IEEE Sens. J.* **13** 4940

[48] Kim S H, Yoon J, Yun S O, Hwang Y, Jang H S and Ko H C 2013 *Adv. Funct. Mater.* **23** 1375

[49] Hong K, Kim S H, Lee K H and Frisbie C D 2013 *Adv. Mater.* **25** 3413

[50] Lin Y H, Faber H, Zhao K, Wang Q, Amassian A, McLachlan M and Anthopoulos T D 2013 *Adv. Mater.* **25** 4340

[51] Yang W, Song K, Jung Y, Jeong S and Moon J 2013 *J. Mater. Chem. C* **1** 4275

[52] Zhou J, Wu G, Guo L, Zhu L and Wan Q 2013 *IEEE Electron Dev. Lett.* **34** 888

[53] Seo J S, Jeon J H, Hwang Y H, Park H, Ryu M, Park S H K and Bae B S 2013 *Sci. Rep.* **3** 2085

[54] Hyung G W, Park J, Wang J X, Lee H W, Li Z H, Koo J R, Kwon S J, Cho E S, Kim W Y and Kim Y K 2013 *Jpn. J. Appl. Phys.* **52** 71102

[55] Hsu H H, Chang C Y and Cheng C H 2013 *Phys. Status Solidi-Rapid Res. Lett.* **7** 285

[56] Hsu H H, Chang C Y, Cheng C H, Yu S H, Su C Y and Su C Y 2013 *Solid-State Electron.* **89** 194

[57] Hsu H H, Chang C Y and Cheng C H 2013 *IEEE Electron Dev. Lett.* **34** 768

[58] Münzenrieder N, Petti L, Zysset C, Kinkeldei T, Salvatore G A and Tröster G 2013 *IEEE Trans. Electron Dev.* **60** 2815

[59] Münzenrieder N, Zysset C, Petti L, Kinkeldei T, Salvatore G A and Tröster G 2013 *Solid-State Electron.* **84** 198

[60] Zysset C, Münzenrieder N, Petti L, Büthe L, Salvatore G A and Tröster G 2013 *IEEE Electron Dev. Lett.* **34** 1394

[61] Sharma B K, Jang B, Lee J E, Bae S H, Kim T W, Lee H J, Kim J H and Ahn J H 2013 *Adv. Funct. Mater.* **23** 2024

[62] Dai M K, Lian J T, Lin T Y and Chen Y F 2013 *J. Mater. Chem. C* **1** 5064

[63] Park S, Cho K, Yang K and Kim S 2014 *J. Vac. Sci. Technol. B* **32** 62203

[64] Wee D, Yoo S, Kang Y H, Kim Y H, Ka J W, Cho S Y, Lee C, Ryu J, Yi M H and Jang K S 2014 *J. Mater. Chem. C* **2** 6395

[65] Chen H, Cao Y, Zhang J and Zhou C 2014 *Nat. Commun.* **5** 4097

[66] Xu H, Pang J, Xu M, Li M, Guo Y, Chen Z, Wang L, Zou J, Tao H, Wang L and Peng J 2014 *ECS J. Solid State Sci. Technol.* **3** Q3035

[67] Xu H, Luo D, Li M, Xu M, Zou J, Tao H, Lan L, Wang L, Peng J and Cao Y 2014 *J. Mater. Chem. C* **2** 1255

[68] Lai H C, Pei Z, Jian J R and Tzeng B J 2014 *Appl. Phys. Lett.* **105** 33510

[69] Ok K C, Park S H K, Hwang C S, Kim H, Shin H S, Bae J and Park J S 2014 *Appl. Phys. Lett.* **104** 63508

[70] Nakajima Y, Nakata M, Takei T, Fukagawa H, Motomura G, Tsuji H, Shimizu T, Fujisaki Y, Kurita T and Yamamoto T 2014 *J. Soc. Inf. Disp.* **22** 137

[71] Rim Y S, Chen H, Liu Y, Bae S H, Kim H J and Yang Y 2014 *ACS Nano* **8** 9680

[72] Petti L, Münzenrieder N, Salvatore G A, Zysset C, Kinkeldei T, Büthe L and Tröster G 2014 *IEEE Trans. Electron Dev.* **61** 1085

[73] Münzenrieder N, Voser P, Petti L, Zysset C, Büthe L, Vogt C, Salvatore G A and Tröster G 2014 *IEEE Electron Dev. Lett.* **35** 69

[74] Lee G J, Kim J, Kim J H, Jeong S M, Jang J E and Jeong J 2014 *Semicond. Sci. Technol.* **29** 35003

[75] Li H U and Jackson T N 2015 *IEEE Electron Dev. Lett.* **36** 35

[76] Liu N, Zhu L Q, Feng P, Wan C J, Liu Y H, Shi Y and Wan Q 2015 *Sci. Rep.* **5** 18082

[77] Kim J, Jeong S M and Jeong J 2015 *Jpn. J. Appl. Phys.* **54** 114102

[78] Honda W, Harada S, Ishida S, Arie T, Akita S and Takei K 2015 *Adv. Mater.* **27** 4674

[79] Jo J W, Kim J, Kim K T, Kang J G, Kim M G, Kim K H, Ko H, Kim Y H and Park S K 2015 *Adv. Mater.* **27** 1182

[80] Motomura G, Nakajima Y, Takei T, Tsuzuki T, Fukagawa H, Nakata M, Tsuji H, Shimizu T, Morii K, Hasegawa M, Fujisaki Y and Yamamoto T 2015 *ITE Trans. Media Technol. Appl.* **3** 121

[81] Jung S W, Koo J B, Park C W, Na B S, Oh J Y, Lee S S and Koo K W 2015 *J. Vac. Sci. Technol. B* **33** 51201

[82] Jin S H, Kang S K, Cho I T, Han S Y, Chung H U, Lee D J, Shin J, Baek G W, Kim T, Lee J H and Rogers J A 2015 *ACS Appl. Mater. Interfaces* **7** 8268

[83] Park M J, Yun D J, Ryu M K, Yang J H, Pi J E, Kwon O S, Kim G H, Hwang C S, Bak J Y and Yoon S M 2015 *J. Mater. Chem. C* **3** 4779

[84] Petti L, Frutiger A, Münzenrieder N, Salvatore G A, Büthe L, Vogt C, Cantarella G and Tröster G 2015 *IEEE Electron Dev. Lett.* **36** 475

[85] Tripathi A K, Myny K, Hou B, Wezenberg K and Gelinck G H 2015 *IEEE Trans. Electron Dev.* **62** 4063

[86] Hsu H H, Chiu Y C, Chiou P and Cheng C H 2015 *J. Alloys Compd.* **643 Supplement 1** S133

[87] Li Y S, He J C, Hsu S M, Lee C C, Su D Y, Tsai F Y and Cheng I C 2016 *IEEE Electron Dev. Lett.* **37** 46

[88] Zhang Y, Mei Z, Cui S, Liang H, Liu Y and Du X 2016 *Adv. Electron. Mater.* **2** 1500486

[89] Zhang L R, Huang C Y, Li G M, Zhou L, Wu W J, Xu M, Wang L, Ning H L, Yao R H and Peng J B 2016 *IEEE Trans. Electron Dev.* **63** 1779

[90] Wang B, Yu X, Guo P, Huang W, Zeng L, Zhou N, Chi L, Bedzyk M J, Chang R P H, Marks T J and Facchetti A 2016 *Adv. Electron. Mater.* **2** 1500427

[91] Park C B, Na H I, Yoo S S and Park K S 2016 *Appl. Phys. Express* **9** 31101

[92] Jung S W, Choi J S, Park J H, Koo J B, Park C W, Na B S, Oh J Y, Lim S C, Lee S S and Chu H Y 2016 *J. Nanosci. Nanotechnol.* **16** 2752

[93] Kim J, Kim J, Jo S, Kang J, Jo J W, Lee M, Moon J, Yang L, Kim M G, Kim Y H and Park S K 2016 *Adv. Mater.* **28** 3078

[94] Oh H, Cho K, Park S and Kim S 2016 *Microelectron. Eng.* **159** 179

[95] Zeumault A, Ma S and Holbery J 2016 *Phys. Status Solidi A* **213** 2189

[96] Nakata M, Motomura G, Nakajima Y, Takei T, Tsuji H, Fukagawa H, Shimizu T, Tsuzuki T, Fujisaki Y and Yamamoto T 2016 *J. Soc. Inf. Disp.* **24** 3

[97] Narushima S, Mizoguchi H, Shimizu K, Ueda K, Ohta H, Hirano M, Kamiya T and Hosono H 2003 *Adv. Mater.* **15** 1409

[98] Schein F L, Wenckstern H von and Grundmann M 2013 *Appl. Phys. Lett.* **102** 92109

[99] Schein F L, Winter M, Böntgen T, Wenckstern H von and Grundmann M 2014 *Appl. Phys. Lett.* **104** 22104

[100] Schlupp P, Schein F L, von Wenckstern H and Grundmann M 2015 *Adv. Electron. Mater.* **1** 1400023

[101] Chen W C, Hsu P C, Chien C W, Chang K M, Hsu C J, Chang C H, Lee W K, Chou W F, Hsieh H H and Wu C C 2014 *J. Phys. Appl. Phys.* **47** 365101

[102] Pal B N, Sun J, Jung B J, Choi E, Andreou A G and Katz H E 2008 *Adv. Mater.* **20** 1023

[103] Brillson L J, Dong Y, Tuomisto F, Svensson B G, Kuznetsov A Y, Doutt D, Mosbacker H L, Cantwell G, Zhang J, Song J J, Fang Z Q and Look D C 2012 *J. Vac. Sci. Technol. B* **30** 50801

[104] Brillson L J and Lu Y 2011 *J. Appl. Phys.* **109** 121301

[105] Chasin A, Nag M, Bhoolokam A, Myny K, Steudel S, Schols S, Genoe J, Gielen G and Heremans P 2013 *IEEE Trans. Electron Dev.* **60** 3407

[106] Zhang J, Li Y, Zhang B, Wang H, Xin Q and Song A 2015 *Nat. Commun.* **6** 7561

[107] Sugimura T, Tsuzuku T, Kasai Y, Iiyama K and Takamiya S 2000 *Jpn. J. Appl. Phys.* **39** 4521

[108] Hemour S and Wu K 2014 *Proc. IEEE* **102** 1667

[109] Grover S and Moddel G 2011 *IEEE J. Photovolt.* **1** 78

[110] Kimura Y, Sun Y, Maemoto T, Sasa S, Kasai S and Inoue M 2013 *Jpn. J. Appl. Phys.* **52** 06GE09

[111] Lee D 2016 CES 2016: Hands-on with LG's roll-up flexible screen, January 5, 2016, *BBC News*

[112] Cervant E 2015 Report: flexible displays will dominate the future with foldable, rollable and even stretchable panels, September 8, 2015, Android Auth.

[113] Park J S, Maeng W J, Kim H S and Park J S 2012 *Thin Solid Films* **520** 1679

[114] Choi C H, Lin L Y, Cheng C C and Chang C 2015 *ECS J. Solid State Sci. Technol.* **4** P3044

[115] Rim Y S, Bae S H, Chen H, De Marco N and Yang Y 2016 *Adv. Mater.* **28** 4415

[116] Harris K D, Elias A L and Chung H J 2015 *J. Mater. Sci.* **51** 2771

[117] Ni H, Liu J, Wang Z and Yang S 2015 *J. Ind. Eng. Chem.* **28** 16

[118] Chien C W, Wu C H, Tsai Y T, Kung Y C, Lin C Y, Hsu P C, Hsieh H H, Wu C C, Yeh Y H, Leu C M and Lee T M 2011 *IEEE Trans. Electron Dev.* **58** 1440

[119] Cantarella G, Münzenrieder N, Petti L, Vogt C, Büthe L, Salvatore G A, Daus A and Tröster G 2015 *IEEE Electron Dev. Lett.* **36** 781

[120] Rogers J A, Someya T and Huang Y 2010 *Science* **327** 1603

[121] Wagner S, Lacour S P, Jones J, Hsu P I, Sturm J C, Li T and Suo Z 2004 *Phys. E Low-Dimens. Syst. Nanostructures* **25** 326

[122] Sekitani T and Someya T 2012 *MRS Bull.* **37** 236

[123] http://www.corning.com/in/en/products/display-glass/products/corning-willow-glass.html

[124] Leterrier Y 2003 *Prog. Mater. Sci.* **48** 1

[125] Knez M, Nielsch K and Niinistö L 2007 *Adv. Mater.* **19** 3425

[126] Kim H, Lee H B R and Maeng W J 2009 *Thin Solid Films* **517** 2563

[127] Münzenrieder N, Salvatore G A, Petti L, Zysset C, Büthe L, Vogt C, Cantarella G and Tröster G 2014 *Appl. Phys. Lett.* **105** 263504

[128] Kamiya T, Nomura K and Hosono H 2009 *J. Disp. Technol.* **5** 273

[129] Dehuff N L, Kettenring E S, Hong D, Chiang H Q, Wager J F, Hoffman R L, Park C H and Keszler D A 2005 *J. Appl. Phys.* **97** 64505

[130] Chiang H Q, Wager J F, Hoffman R L, Jeong J and Keszler D A 2005 *Appl. Phys. Lett.* **86** 13503

[131] Jackson W B, Hoffman R L and Herman G S 2005 *Appl. Phys. Lett.* **87** 193503

[132] Janotti A and Van de Walle C G 2009 *Rep. Prog. Phys.* **72** 126501

[133] Janotti A and Walle C G V de 2005 *Appl. Phys. Lett.* **87** 122102

[134] Liu L, Mei Z, Tang A, Azarov A, Kuznetsov A, Xue Q K and Du X 2016 *Phys. Rev. B* **93** 235305

[135] Suresh A, Wellenius P, Dhawan A and Muth J 2007 *Appl. Phys. Lett.* **90** 123512

[136] Saji K J, Jayaraj M K, Nomura K, Kamiya T and Hosono H 2008 *J. Electrochem. Soc.* **155** H390

[137] Jeon I Y, Lee J Y and Yoon D H 2013 *J. Nanosci. Nanotechnol.* **13** 1741

[138] Kim K A, Bak J Y, Choi J S and Yoon S M 2014 *Ceram. Int.* **40** 7829

[139] Lee Y G and Choi W S 2013 *Electron. Mater. Lett.* **9** 719

[140] Chong E, Jo K C and Lee S Y 2010 *Appl. Phys. Lett.* **96** 152102

[141] Kim C J, Kim S, Lee J H, Park J S, Kim S, Park J, Lee E, Lee J, Park Y, Kim J H, Shin S T and Chung U I 2009 *Appl. Phys. Lett.* **95** 252103

[142] Park J S, Kim K, Park Y G, Mo Y G, Kim H D and Jeong J K 2009 *Adv. Mater.* **21** 329

[143] Chong E, Kim S H and Lee S Y 2010 *Appl. Phys. Lett.* **97** 252112

[144] Chong E, Chun Y S and Lee S Y 2010 *Appl. Phys. Lett.* **97** 102102

[145] Noh J, Jung M, Jung Y, Yeom C, Pyo M and Cho G 2015 *Proc. IEEE* **103** 554

[146] Subramanian V, Cen J, Vornbrock A de la F, Grau G, Kang H, Kitsomboonloha R, Soltman D and Tseng H Y 2015 *Proc. IEEE* **103** 567

[147] Grau G and Subramanian V 2016 *Adv. Electron. Mater.* **2** 1500328

[148] Lim N, Kim J, Lee S, Kim N and Cho G 2009 *IEEE Trans. Adv. Packag.* **32** 72

[149] Sekitani T, Nakajima H, Maeda H, Fukushima T, Aida T, Hata K and Someya T 2009 *Nat. Mater.* **8** 494

[150] Chang J B, Liu V, Subramanian V, Sivula K, Luscombe C, Murphy A, Liu J and Fréchet J M J 2006 *J. Appl. Phys.* **100** 14506

[151] Niinistö L, Nieminen M, Päiväsaari J, Niinistö J, Putkonen M and Nieminen M 2004 *Phys. Status Solidi A* **201** 1443

[152] Jen S H, Bertrand J A and George S M 2011 *J. Appl. Phys.* **109** 84305

[153] Pecunia V, Banger K and Sirringhaus H 2015 *Adv. Electron. Mater.* **1** 1400024

[154] Facchetti A, Yoon M H and Marks T J 2005 *Adv. Mater.* **17** 1705

[155] Kim D H, Choi S H, Cho N G, Chang Y, Kim H G, Hong J M and Kim I D 2009 *Electrochem. Solid-State Lett.* **12** H296

[156] Hwang B U, Kim D I, Cho S W, Yun M G, Kim H J, Kim Y J, Cho H K and Lee N E 2014 *Org. Electron.* **15** 1458

[157] Shannon R D 1993 *J. Appl. Phys.* **73** 348

[158] Han W, Lee H S, Bangi U K H, Yoo B and Park H H 2016 *Polym. Adv. Technol.* **27** 245

[159] Chen R, Kim H, McIntyre P C and Bent S F 2005 *Chem. Mater.* **17** 536

[160] Lee J P, Jang Y J and Sung M M 2003 *Adv. Funct. Mater.* **13** 873

[161] Minami T 2005 *Semicond. Sci. Technol.* **20** S35

[162] Pasquarelli R M, Ginley D S and O'Hayre R 2011 *Chem. Soc. Rev.* **40** 5406

[163] Leterrier Y, Médico L, Demarco F, Månson J A E, Betz U, Escolà M F, Kharrazi Olsson M and Atamny F 2004 *Thin Solid Films* **460** 156

[164] Kim Y S, Hwang W J, Eun K T and Choa S H 2011 *Appl. Surf. Sci.* **257** 8134

[165] Park Y S, Kim H K, Jeong S W and Cho W J 2010 *Thin Solid Films* **518** 3071

[166] Ko Y D, Lee C H, Moon D K and Kim Y S 2013 *Thin Solid Films* **547** 32

[167] Bender M, Seelig W, Daube C, Frankenberger H, Ocker B and Stollenwerk J 1998 *Thin Solid Films* **326** 67

[168] Park Y S, Choi K H, Kim H K and Kang J W 2010 *Electrochem. Solid-State Lett.* **13** J39

[169] Park Y S and Kim H K 2010 *J. Vac. Sci. Technol. A* **28** 41

[170] Kim H K and Lim J W 2012 *Nanoscale Res. Lett.* **7** 67

[171] Cho S W, Jeong J A, Bae J H, Moon J M, Choi K H, Jeong S W, Park N J, Kim J J, Lee S H, Kang J W, Yi M S and Kim H K 2008 *Thin Solid Films* **516** 7881

[172] Park Y S, Choi K H and Kim H K 2009 *J. Phys. Appl. Phys.* **42** 235109

[173] Park Y S, Park H K, Jeong J A, Kim H K, Choi K H, Na S I and Kim D Y 2009 *J. Electrochem. Soc.* **156** H588

[174] Choi K H, Nam H J, Jeong J A, Cho S W, Kim H K, Kang J W, Kim D G and Cho W J 2008 *Appl. Phys. Lett.* **92** 223302

[175] Park H K, Jeong J A, Park Y S, Na S I, Kim D Y and Kim H K 2009 *Electrochem. Solid-State Lett.* **12** H309

[176] Choi Y Y, Kim H K, Koo H W, Kim T W and Lee S N 2011 *J. Vac. Sci. Technol. A* **29** 61502

[177] Lim J W, Oh S I, Eun K, Choa S H, Koo H W, Kim T W and Kim H K 2012 *Jpn. J. Appl. Phys.* **51** 115801

[178] Lee J, Lee P, Lee H, Lee D, Lee S S and Ko S H 2012 *Nanoscale* **4** 6408

[179] Yu Z, Zhang Q, Li L, Chen Q, Niu X, Liu J and Pei Q 2011 *Adv. Mater.* **23** 664

[180] Lim J W, Cho D Y, Eun K, Choa S H, Na S I, Kim J and Kim H K 2012 *Sol. Energy Mater. Sol. Cells* **105** 69

[181] Lee J Y, Connor S T, Cui Y and Peumans P 2008 *Nano Lett.* **8** 689

[182] Hu L, Kim H S, Lee J Y, Peumans P and Cui Y 2010 *ACS Nano* **4** 2955

[183] Zhang K, Han K, Shi S, Bahl G and Tawfick S 2016 *Adv. Electron. Mater.* **2** 1600003

[184] Kim H J and Kim Y J 2014 *IOP Conf. Ser. Mater. Sci. Eng.* **62** 12022

[185] Lee M H, Hsu S M, Shen J D and Liu C 2015 *Microelectron. Eng.* **138** 77

[186] Dauzou F, Bouten P C P, Dabirian A, Leterrier Y, Ballif C and Morales-Masis M 2016 *Org. Electron.* **35** 136

[187] Gleskovas H, Wagner S and Suo Z 1999 *MRS Online Proceedings Library Archive* **557** p. 653

[188] Gleskova H, Wagner S and Suo Z 1999 *Appl. Phys. Lett.* **75** 3011

[189] Suo Z, Ma E Y, Gleskova H and Wagner S 1999 *Appl. Phys. Lett.* **74** 1177

[190] Sekitani T, Iba S, Kato Y, Noguchi Y, Someya T and Sakurai T 2005 *Appl. Phys. Lett.* **87** 173502

[191] Park S K, Han J I, Moon D G and Kim W K 2003 *Jpn. J. Appl. Phys.* **42** 623

[192] Gleskova H, Wagner S and Suo Z 2000 *J. Non-Cryst. Solids* **266–269, Part 2** 1320

[193] Chen B W, Chang T C, Hung Y J, Hsieh T Y, Tsai M Y, Liao P Y, Chen B Y, Tu Y H, Lin Y Y, Tsai W W and Yan J Y 2015 *Appl. Phys. Lett.* **106** 183503

[194] Munzenrieder N, Cherenack K H and Troster G 2011 *IEEE Trans. Electron Dev.* **58** 2041

[195] Heremans P, Tripathi A K, de Jamblinne de Meux A, Smits E C P, Hou B, Pourtois G and Gelinck G H 2016 *Adv. Mater.* **28** 4266

[196] Rockett A 2008 *The Materials Science of Semiconductors* (Springer US) pp. 195–235

[197] Song K, Young Koo C, Jun T, Lee D, Jeong Y and Moon J 2011 *J. Cryst. Growth* **326** 23

[198] Yoo Y B, Park J H, Lee S J, Song K M and Baik H K 2012 *Jpn. J. Appl. Phys.* **51** 40201

[199] Hwang Y H, Kim K S and Cho W J 2014 *Jpn. J. Appl. Phys.* **53** 04EF12

[200] Moon S W and Cho W J 2015 *J. Semicond. Technol. Sci.* **15** 249

[201] Oh S M, Jo K W and Cho W J 2015 *Curr. Appl. Phys.* **15, Supplement 2**

[202] Hwang Y H, Seo S J, Jeon J H and Bae B S 2012 *Electrochem. Solid-State Lett.* **15** H91

[203] Yang Y H, Yang S S and Chou K S 2010 *IEEE Electron Dev. Lett.* **31** 969

[204] Park J, Kim C S, Ahn B D, Ryu H and Kim H S 2015 *J. Electroceramics* **35** 106